Coupled Systems Mechanics, *Vol. 7, No. 5 (2018) 525-554*
DOI: https://doi.org/10.12989/csm.2018.7.5.525

Dynamics of the system consisting of the hollow cylinder and surrounding infinite elastic medium under action an oscillating moving ring load on the interior of the cylinder

Surkay D. Akbarov[*1,2] and Mahir A. Mehdiyev[2,3a]

[1]*Yildiz Technical University, Faculty of Mechanical Engineering, Department of Mechanical Engineering, Yildiz Campus, 34349, Besiktas, Istanbul-Turkey*
[2]*Institute of Mathematics and Mechanics of National Academy of Science of Azerbaijan, 37041, Baku, Azerbaijan*
[3]*Azerbaijan State Economic University, Department of Mathematics, Baku, Azerbaijan*

(Received January 8, 2018, Revised May 2, 2018, Accepted May 4, 2018)

Abstract. The paper deals with the study of the dynamics of the oscillating moving ring load acting in the interior of the hollow circular cylinder surrounded by an elastic medium. The axisymmetric loading case is considered and the study is made by employing the exact equations and relations of linear elastodynamics. The focus is on the influence of the oscillation of the moving load and the problem parameters such as the cylinder's thickness/radius ratio on the critical velocities. At the same time, the dependence between the interface stresses and load moving velocity under various frequencies of this load, as well as the frequency response of the mentioned stresses under various load velocity are investigated. In particular, it is established that oscillation of the moving load can cause the values of the critical velocity to decrease significantly and at the same time the oscillation of the moving load can lead to parametric resonance. It is also established that the critical velocity decreases with decreasing of the cylinder's thickness/radius ratio.

Keywords: critical velocity; oscillating moving load; frequency response; parametric resonance; stress distribution

1. Introduction

The study of the fundamental problems related to the dynamics of the oscillating moving load acting in the elastic and viscoelastic systems consisting of hollow cylinder and surrounding elastic or viscoelastic medium is required in line with the development and successful application of modern high-speed underground trains and other types of underground moving wheels. This is because, in studies, underground structures into which such high-speed wheels move are modelled as infinite hollow cylinders surrounded by an elastic or viscoelastic medium.

It should be noted that one of the main dynamical characteristics of the systems subjected to the action of a moving load is its critical velocity under which resonance type behavior of the system

*Corresponding author, Professor, E-mail: akbarov@yildiz.edu.tr
[a]Associate Professor, E-mail: mahirmehdiyev@mail.ru

http://www.techno-press.org/?journal=csm&subpage=8 ISSN: 2234-2184 (Print), 2234-2192 (Online)

takes place. In connection with this, the main issue in related investigations is determination of both the critical velocity and the influence of the problem parameters on the values of this velocity. At the same time, another issue which is also important is to determine the rules of attenuation of the perturbations of the stresses and displacements caused by the moving load with the distance from the point at which this load acts. Namely, the investigations of these issues for the bi-material layered system "hollow cylinder + surrounding infinite elastic medium" under action of the oscillating moving load is the subject of the present paper. In order to determine the place and significance of the investigations presented, we consider a brief review of the corresponding investigations regarding layered elastic systems. Note that a review of investigations related to the action of the moving load on beams, plates and other types of elements of construction, has been made by Ouyang (2011).

Thus, we begin this review with the paper by Achenbach *et al*. (1967) in which the dynamic response of the system consisting of the covering layer and half plane to a moving load was investigated with the use of the Timoshenko theory for describing the motion of the plate. However, the motion of the half-plane was described by using the exact equations of the theory of linear elastodynamics and the plane-strain state was considered. It is established that the critical velocity exists in the cases where the plate material is stiffer than that of the half-plane material. A review of later investigations, which can be taken as developments of those started in the paper by Achenbach *et al*. (1967), are described in the papers by Dieterman and Metrikine (1997) and Metrikine and Vrouwenvelder (2000). Note that in the paper by Dieterman and Metrikine (1997), it is established that the time harmonic variety of the moving load causes two types of critical velocities to appear: The first (the second) of which is lower (higher) than the Rayleigh wave velocity in the plate material. Later, similar results were also obtained by Akbarov and Salmanova (2009), Akbarov and Ilhan (2009), Akbarov *et al*. (2015) and others, which are also discussed in the monograph by Akbarov (2015). However, in the latter works the foregoing results on the influence of the time harmonic variety of the moving load on the critical velocity is formulated as follows: As a result of the noted-above variety, two types of critical velocity appear, the first (second) of which is less (greater) than that obtained for the corresponding constant moving load. Moreover, in later works, initially stressed layered systems are considered and the influence of these stresses on the values of the critical velocity is also investigated. There are also series of investigations related to the dynamics of the moving load with constant velocity acting on the pre-stressed layered systems which include investigations by Akbarov *et al*. (2007), Akbarov and Ilhan (2008), Dincsoy *et al*. (2009), Babich *et al*. (1986, 1988, 2008a, 2008b) and others. At the same time, the dynamics of the moving and of the oscillating moving load acting on the hydro-elastic systems consisting of the plate and compressible viscous fluid are investigated in the papers by Akbarov and Ismailov (2015, 2016a), Akbarov and Panakhli (2015, 2017) and Akbarov, Ismailov and Aliyev (2017).

The effect of imperfect bonding on the axisymmetric elastodynamic response of the system consisting of isotropic hollow cylinder and surrounding poroelastic soil due to a moving ring load is studied by Hasheminejad and Komeili (2009). As in the above reviewed works, the steady-state case is considered and the character of the influence of the bonding conditions on the critical velocity and radial displacement of the cylinder is established.

The influence of the poroelasticity of the subgrade material on the dynamic response on the moving load acting on a Bernoulli-Euler beam supported with this subgrade material is investigated by Shi and Selvadurai (2016) by employing the concept of the equivalent stiffness of the half-space. Note that in this investigation, as the viscosity of the beam is taken into consideration, the critical velocities are defined as the velocities at which the beam displacement under the load reaches a maximum. It is established that for the system under consideration there exist two types of critical velocities. The first refers to the case where the equivalent stiffness of the half-space is zero. However, the second which is slightly less than the corresponding first critical velocity is determined from the peak values of the beam displacements.

The paper by Zhenning *et al*. (2016) studies the 3D steady-state dynamic response of the multi-layered transversely isotropic half-space generated by a point-located moving load with constant velocity acting on the face plane of this half plane. It is assumed that the packet of layers made of hysteretic viscoelastic transversely isotropic materials lies on a half-space which is also made from a hysteretic viscoelastic transversely isotropic material. Numerical results on the influence of the materials' anisotropy on the critical velocities, stress and displacement distributions are presented and discussed.

Now we consider a review of the investigations related to the dynamics of the moving load acting in the interior of the cylindrical bore (cavity) with infinite length within the infinite homogeneous and cylindrically layered medium. Apparently, the first attempt in this field was made by Parnes (1969) in which a line load applied along a transverse circle moving with constant velocity in the axial direction along the interior of a circular bore in an infinite homogeneous elastic medium is investigated. The supersonic regime is considered, i.e., it is assumed that the velocity of the moving load is greater than the shear and longitudinal waves' velocities in the elastic medium. The 3D problem in the cylindrical coordinate system is considered and the numerical results on the stress and displacements are presented only for the axisymmetric case. Later, in another paper by Parnes (1980), the problem noted above is considered for the case where in the interior of the cylindrical cavity a torsional moving load acts. However, in these papers the question related to the critical velocity is not considered. This is because the critical velocity of the moving load acting on infinite (as in the papers by Parnes (1969, 1980)) or semi-infinite mediums does not appear in the cases where these mediums are homogeneous. Consequently, the question related to determination of the critical velocity relates only to moving load problems acting on the piece-wise inhomogeneous infinite (for instance, for the system consisting of a hollow cylinder surrounded with elastic medium) or semi-infinite (for instance, for the system consisting of a covering layer and half-space) bodies. What is more, the critical velocity in the aforementioned infinite and semi-infinite bodies appears only in the cases where the modulus of elasticity of the covering layer material is greater than that of the surrounding infinite medium or of the stratified semi-infinite medium. Note that the investigations carried out in the papers by Chonan (1981), Pozhuev (1980), Abdulkadirov (1981) and others relate to the piece-wise inhomogeneous infinite cylindrically layered systems.

Chonan (1981) studies the dynamic response of a cylindrical shell imperfectly bonded to a surrounding infinite elastic continuum under action of axisymmetric ring pressure which moves with constant velocity in the axial direction along the interior of the shell. The subsonic regime is considered and it is assumed that the shell and the continuum are joined together by a thin elastic bond. The axisymmetric problem is considered and the motion of the shell is described by thick shell theories and the motion of the surrounding elastic medium is described by the exact equations of linear elastodynamics. The numerical results on the critical speed of the moving load and the influence of the problem parameters on this velocity are presented and discussed. Moreover, the numerical results related to the radial displacement of the shell for the subcritical moving load are presented.

In the paper by Pozhuev (1980), the moving load problem is studied for the system consisting of a thin cylindrical shell and surrounding transversally isotropic infinite medium. The motion of the cylinder is described by a thin shell theory and the motion of the surrounding elastic medium is described with the exact equations of motion of elastodynamics for transversally isotropic bodies. Numerical results regarding displacements and a radial normal stress are presented. However, in the paper by Pozhuev (1980) there are no numerical results related to the critical velocity of the moving load.

The paper by Abdulkadirov (1981) deals with the study of low-frequency resonance axisymmetric longitudinal waves in a cylindrical layer surrounded by an elastic medium. Note that under "resonance waves" the cases under which the relation $dc/dk = 0$ occurs, is understood, where c is the wave propagation velocity and k is the wavenumber. It is evident that the velocity of these "resonance waves" is the critical velocity of the corresponding moving load. Some numerical examples of "resonance waves" are presented and discussed. It should be noted that under obtaining dispersion curves, the motion of the hollow cylinder and surrounding elastic medium is described through the exact equations of linear elastodynamics.

Another example of investigations related to the problems of the moving load acting on the cylindrical layered system is the investigation carried out in the paper by Zhou *et al*. (2008) in which the critical velocity of the moving internal pressure acting in the sandwich shell is studied. Under this investigation, two types of approaches were used, the first of which is based on first order refined sandwich shell theories, while the second approach is based on the exact equations of linear elastodynamics for orthotropic bodies with effective mechanical constants, the values of which are determined by the well-known expressions through the values of the mechanical constants and volumetric fraction of each layer of the sandwich shell. Numerical results on the critical velocity obtained within these approaches are presented and discussed. Comparison of the corresponding results obtained by these approaches shows that they are sufficiently close to each other for the low wavenumber cases, however, the difference between these results increases with the wavenumber and becomes so great that it appears necessary to determine which approach is more accurate. It is evident that for this determination it is necessary to investigate these problems by employing the exact field equations of elastodynamics within the scope of the piecewise homogeneous body model, which is also used in the present paper.

In recent years in the papers by Forrest and Hunt (2006), Sheng *et al*. (2006), Hung *et al*. (2013), Hussein *et al*. (2014), Yuan *et al*. (2017) and others listed therein, numerical and analytical solution methods have been developed for studying the dynamical response of tunnel (modelled as a hollow elastic cylinder) + soil (modeled as surrounding elastic or viscoelastic medium) systems generated by the moving load acting on the interior of the tunnels. However, the focus in these investigations is on the displacement distribution of the soils caused by the moving load.

With this we restrict ourselves to the review of related investigations from which it follows that up to now systematic investigations of the critical velocity of a moving load acting on the interior of the hollow cylinder surrounded with elastic medium are absent. The first attempt in this field is made in the work by Akbarov and Mehdiyev (2017a) in which the dynamics of the moving ring load acting in the interior of the pre-stressed cylinder surrounded with the pre-stressed elastic medium is studied. Moreover, in the paper by Akbarov and Mehdiyev (2017b) the dynamics of the time-harmonic ring load acting also in the interior of the hollow cylinder which is surrounded with elastic medium is investigated. Note that in these papers the axisymmetric problems are considered. However, up to now the investigations related to the critical velocity of the oscillating moving load, also acting on the interior of the hollow cylinder surrounded by elastic medium, are almost completely absent. Note that such investigations have a great significance not only in the

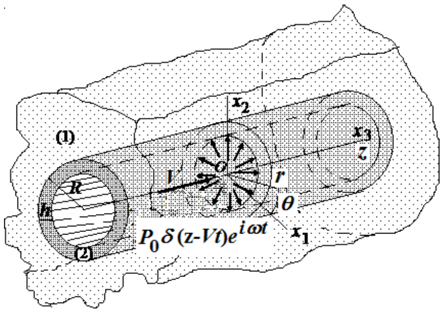

Fig. 1 The sketch of the system under consideration and the oscillating moving ring load

theoretical, but also in the practical sense. This is because any underground moving wheel has an oscillation with a certain frequency and knowledge of the influence of this oscillation on the critical velocity of the moving ring forces can prevent many catastrophic accidents. Taking this statement into consideration in the present paper some attempts are made in this field and the critical velocity of the oscillating moving ring load acting in the interior of the hollow cylinder surrounded with infinite elastic medium is investigated. At the same time, in the present paper for the subcritical moving velocities, the distribution of the interface normal and shear stresses is also studied. Corresponding investigations are made for the axisymmetric case and the exact equations and relations of linear elastodynamics are employed and it is assumed that the moving velocity of the load is subsonic. Numerical results on the influence of the problem parameters and of the oscillation frequency of the moving ring load on the critical velocities and on the stress distributions are presented and discussed.

2. Formulation of the problem

Consider a hollow circular cylinder with thickness h which is surrounded by an infinite elastic medium and associate the cylindrical and Cartesian systems of coordinates $Or\theta z$ and $Ox_1x_2x_3$ (Fig. 1) with the central axis of this cylinder.

Assume that the external radius of the cross section of the cylinder is R and on the inner surface of this cylinder normal time-harmonic ring forces act and these forces move along the cylinder axis with constant velocity V. Within this framework, we investigate the axisymmetric stress-strain state in this system by employing the exact equations of the linear theory of elastodynamics within the scope of the piecewise homogeneous body model. Below, we will use the upper indices (2) and (1) to denote the values related to the cylinder and to the surrounding elastic medium, respectively.

Assuming that the materials of the constituents are homogeneous and isotropic we write the field equations and boundary and contact conditions.

Equations of motion

$$\frac{\partial\sigma_{rr}^{(k)}}{\partial r}+\frac{\partial\sigma_{rz}^{(k)}}{\partial z}+\frac{1}{r}(\sigma_{rr}^{(k)}-\sigma_{\theta\theta}^{(k)})=\rho^{(k)}\frac{\partial^2 u_r^{(k)}}{\partial t^2},$$
$$\frac{\partial\sigma_{rz}^{(k)}}{\partial r}+\frac{\partial\sigma_{zz}^{(k)}}{\partial z}+\frac{1}{r}\sigma_{rz}^{(k)}=\rho^{(k)}\frac{\partial^2 u_z^{(k)}}{\partial t^2} \qquad (1)$$

Elasticity relations

$$\sigma_{nn}^{(k)} = \lambda^{(k)}(\varepsilon_{rr}^{(k)} + \varepsilon_{\theta\theta}^{(k)} + \varepsilon_{zz}^{(k)}) + 2\mu^{(k)}\varepsilon_{nn}^{(k)}, \quad nn = rr;\theta\theta;zz \quad , \quad \sigma_{rz}^{(k)} = 2\mu^{(k)}\varepsilon_{rz}^{(k)} \tag{2}$$

Strain-displacement relations

$$\varepsilon_{rr}^{(k)} = \frac{\partial u_r^{(k)}}{\partial r}, \quad \varepsilon_{\theta\theta}^{(k)} = \frac{u_r^{(k)}}{r} \quad , \quad \varepsilon_{zz}^{(k)} = \frac{\partial u_z^{(k)}}{\partial z}, \quad \varepsilon_{rz}^{(k)} = \frac{1}{2}(\frac{\partial u_z^{(k)}}{\partial r} + \frac{\partial u_r^{(k)}}{\partial z}) \tag{3}$$

The equations (1), (2) and (3) are the complete system of field equations of the linear theory of elastodynamics in the case under consideration and in these equations conventional notation is used.

Consider the formulation of the boundary and contact conditions. According to the foregoing description of the problem, the boundary conditions in the inner face surface of the cylinder can be formulated as follows

$$\sigma_{rr}^{(2)}\Big|_{r=R-h} = -P_0\delta(z-Vt)e^{i\omega t}, \quad \sigma_{rz}^{(2)}\Big|_{r=R-h} = 0 \tag{4}$$

Suppose that the contact conditions with respect to the forces and radial displacement are continuous and can be written as follows

$$\sigma_{rr}^{(1)}\Big|_{r=R} = \sigma_{rr}^{(2)}\Big|_{r=R}, \sigma_{rz}^{(1)}\Big|_{r=R} = \sigma_{rz}^{(2)}\Big|_{r=R}, \quad u_r^{(1)}\Big|_{r=R} = u_r^{(2)}\Big|_{r=R} \quad . \quad u_z^{(1)}\Big|_{r=R} = u_z^{(2)}\Big|_{r=R}. \tag{5}$$

Besides all these, we assume that

$$\left|\sigma_{rr}^{(1)}\right|;\left|\sigma_{\theta\theta}^{(1)}\right|;\left|\sigma_{zz}^{(1)}\right|;\left|\sigma_{rz}^{(1)}\right|;\left|u_r^{(1)}\right|;\left|u_z^{(1)}\right| < M = const. \text{ as } \sqrt{r^2+z^2} \to \infty. \tag{6}$$

This completes formulation of the problem and consideration of the governing field equations.

3. Method of solution

We use the well-known, classical Lame (or Helmholtz) decomposition (see, for instance, the monograph by Eringen and Suhubi (1975) and others listed therein) for solution of the above formulated problem

$$u_r^{(k)} = \frac{\partial \Phi^{(k)}}{\partial r} + \frac{\partial^2 \Psi^{(k)}}{\partial r \partial z}, \quad u_z^{(k)} = \frac{\partial \Phi^{(k)}}{\partial z} + \frac{\partial^2 \Psi^{(k)}}{\partial r^2} + \frac{1}{r}\frac{\partial \Psi^{(k)}}{\partial r}, \tag{7}$$

where $\Phi^{(k)}$ and $\Psi^{(k)}$ satisfy the following equations

$$\nabla^2\Phi^{(k)} - \frac{1}{(c_1^{(k)})^2}\frac{\partial^2\Phi^{(k)}}{\partial t^2} = 0, \quad \nabla^2\Psi^{(k)} - \frac{1}{(c_2^{(k)})^2}\frac{\partial^2\Psi^{(k)}}{\partial t^2} = 0, \quad \nabla^2 = \frac{\partial^2}{\partial r^2} + \frac{1}{r}\frac{\partial}{\partial r} + \frac{\partial^2}{\partial z^2}, \tag{8}$$

where $c_1^{(k)} = \sqrt{(\lambda^{(k)} + \mu^{(k)})/\rho^{(k)}}$ and $c_2^{(k)} = \sqrt{\mu^{(k)}/\rho^{(k)}}$.

Using the moving coordinate system

$$r' = r, \quad z' = z - Vt \tag{9}$$

which moves with the moving internal pressure, representing all the sought values as $g(r, z', t) = \overline{g}(r, z')e^{i\omega t}$ (below, the over bar and upper prime will be omitted) and rewriting the Eq. (9) with the coordinates r' and z', we obtain

$$\nabla^2\Phi^{(k)} - \frac{1}{(c_1^{(k)})^2}\left(V^2\frac{\partial^2\Phi^{(k)}}{\partial z^2} - 2i\omega V\frac{\partial\Phi^{(k)}}{\partial z} - \omega^2\Phi^{(k)}\right) = 0\,,$$
$$\nabla^2\Psi^{(k)} - \frac{1}{(c_2^{(k)})^2}\left(V^2\frac{\partial^2\Psi^{(k)}}{\partial z^2} - 2i\omega V\frac{\partial\Psi^{(k)}}{\partial z} - \omega^2\Psi^{(k)}\right) = 0\,. \tag{10}$$

After the foregoing transformations, the first condition in (4) transforms to the following one

$$\sigma_{rr}^{(2)}\Big|_{r=R-h} = -P_0\delta(z)\,, \tag{11}$$

but the other relations and conditions in (1)-(6) remain valid for the amplitudes of the sought values in the new coordinates determined by (9).

Below we will use the dimensionless coordinates $\overline{r} = r / h$ and $\overline{z} = z / h$ instead of the coordinates r and z, respectively and the over-bar in $\overline{r}$ and $\overline{z}$ will be omitted.

For solution to the considered boundary value problem we use the exponential Fourier transform, $f_F = \int_{-\infty}^{+\infty} f(z)e^{isz}dz$, according to which, the functions $\Phi^{(k)}$ and $\Psi^{(k)}$ and the amplitudes of the sought values can be presented as follows

$$\left\{\Phi^{(k)};\Psi^{(k)};u_z^{(k)};u_r^{(k)};\sigma_{nn}^{(k)};\sigma_{rz}^{(k)};\varepsilon_{nn}^{(k)};\varepsilon_{rz}^{(k)}\right\}(r,z) = \frac{1}{2\pi}\int_{-\infty}^{\infty}\left\{\Phi_F^{(k)};\Psi_F^{(k)};u_{zF}^{(k)};u_{rF}^{(k)};\sigma_{nnF}^{(k)};\right.$$
$$\left.\sigma_{rzF}^{(k)};\varepsilon_{nnF}^{(k)};\varepsilon_{rzF}^{(k)}\right\}(r,s)e^{-isz}ds\,,\quad nn = rr;\theta\theta;zz\,. \tag{12}$$

Thus, substituting the expressions in (12) into the foregoing equations, relations and contact and boundary conditions, we obtain the corresponding ones for the Fourier transformations of the sought values. Note that after this substitution, the relation (2), the first and second relation in (3), the second condition in (4) and all the conditions in (5) and (6) also remain valid for their Fourier transforms. However, the third and fourth relation in (3), the condition (11) and the relations in (7) transform to the following ones

$$\varepsilon_{zzF}^{(k)} = isu_{zF}^{(k)}\,,\quad \varepsilon_{rzF}^{(k)} = \frac{1}{2}\left(\frac{\partial u_{zF}^{(k)}}{\partial r} - isu_{rF}^{(k)}\right),\quad \sigma_{rrF}^{(2)}\Big|_{r=R-h} = -P_0\,, \tag{13}$$

where, according to the equations in (8), the functions $\Phi_F^{(k)}$ and $\Psi_F^{(k)}$ are determined from the following equations

$$\left[\frac{d^2}{dr^2} + \frac{1}{r}\frac{d}{dr} - \left(s^2 - \frac{W^2(c_2^{(2)})^2}{(c_1^{(k)})^2}\right)\right]\Phi_F^{(k)} = 0\,,\quad \left[\frac{d^2}{dr^2} + \frac{1}{r}\frac{d}{dr} - \left(s^2 - \frac{W^2(c_2^{(2)})^2}{(c_2^{(k)})^2}\right)\right]\Psi_F^{(k)} = 0\,, \tag{14}$$

where

$$W = \Omega - sc\,,\quad \Omega = \frac{\omega h}{c_2^{(2)}}.\quad c = \frac{V}{c_2^{(2)}}. \tag{15}$$

Taking into consideration the conditions in (6), the solution to the equations in (14) are found as follows

$$\begin{gathered}\Phi_F^{(2)} = A_1 H_0^{(1)}(r_1) + A_2 H_0^{(2)}(r_1)\,,\\ \Psi_F^{(2)} = B_1 H_0^{(1)}(r_2) + B_2 H_0^{(2)}(r_2)\,,\\ \Phi_F^{(2)} = C_2 H_0^{(2)}(r_{11})\,,\ \Psi_F^{(2)} = D_2 H_0^{(2)}(r_{21})\,,\end{gathered} \tag{16}$$

where $H_0^{(1)}(x)$ and $H_0^{(2)}(x)$ are the Hankel functions of the first and second kinds, respectively and

$$\begin{gathered} r_1 = r\sqrt{W^2\delta_1^2 - s^2}\,,\ \delta_1 = \frac{c_2^{(2)}}{c_1^{(2)}}\,,\ r_2 = r\sqrt{W^2 - s^2}\,,\\ r_{11} = r\sqrt{W_1^2\delta_2^2 - s^2}\,,\ W_1 = W\frac{c_2^{(2)}}{c_2^{(1)}}\,,\ r_{21} = r\sqrt{W_1^2 - s^2}\,.\end{gathered} \tag{17}$$

Thus, using the solutions in (16), expressions in (13) and the Fourier transformation of the expressions in (2) and (3), we obtain the following expressions for the Fourier transformation of the sought values.

$$u_{rF}^{(2)} = -A_1\frac{dr_1}{dr}H_1^{(1)}(r_1) - A_2\frac{dr_1}{dr}H_1^{(2)}(r_1) + B_1\frac{dr_2}{dr}isH_1^{(1)}(r_2) + B_2\frac{dr_2}{dr}isH_1^{(2)}(r_2)\,,$$

$$u_{zF}^{(2)} = -A_1 isH_0^{(1)}(r_1) - A_2 isH_0^{(2)}(r_1) + B_1(W^2 - s^2)H_0^{(1)}(r_2) + B_2(W^2 - s^2)H_0^{(2)}(r_2)\,,$$

$$\begin{gathered}\sigma_{rrF}^{(2)} = \mu^{(2)}\Big[A_1\Big(-(1+\frac{\lambda^{(2)}}{2\mu^{(2)}})\Big(\frac{dr_1}{dr}\Big)^2 (H_0^{(1)}(r_1) - H_2^{(1)}(r_1)) -\\ \frac{\lambda^{(2)}}{\mu^{(2)}}\frac{dr_1}{dr}H_1^{(1)}(r_1) - \frac{\lambda^{(2)}}{\mu^{(2)}}s^2H_0^{(1)}(r_1)\Big) + A_2\Big(-(1+\frac{\lambda^{(2)}}{2\mu^{(2)}})\Big(\frac{dr_1}{dr}\Big)^2 (H_0^{(2)}(r_1) - H_2^{(2)}(r_1)) -\\ \frac{\lambda^{(2)}}{\mu^{(2)}}\frac{dr_1}{dr}H_1^{(2)}(r_1) - \frac{\lambda^{(2)}}{\mu^{(2)}}s^2H_0^{(2)}(r_1)\Big) + B_1\Big(-(1+\frac{\lambda^{(2)}}{2\mu^{(2)}})\Big(\frac{dr_2}{dr}\Big)^2 is(H_0^{(1)}(r_2) - H_2^{(1)}(r_2)) +\\ \frac{\lambda^{(2)}}{\mu^{(2)}}\frac{1}{r}\frac{dr_2}{dr}isH_1^{(1)}(r_2) - \frac{\lambda^{(2)}}{\mu^{(2)}}is(W^2 - s^2)H_0^{(1)}(r_2)\Big) + B_2\Big(-(1+\frac{\lambda^{(2)}}{2\mu^{(2)}})\Big(\frac{dr_2}{dr}\Big)^2 is(H_0^{(2)}(r_2) - H_2^{(2)}(r_2)) +\\ \frac{\lambda^{(2)}}{\mu^{(2)}}\frac{1}{r}\frac{dr_2}{dr}isH_1^{(2)}(r_2) - \frac{\lambda^{(2)}}{\mu^{(2)}}is(W^2 - s^2)H_0^{(2)}(r_2)\Big)\Big]\,,\end{gathered} \tag{18}$$

$$\sigma_{rzF}^{(2)} = \mu^{(2)}\left[A_1 \frac{dr_1}{dr} 2isH_1^{(1)}(r_1) + A_2 \frac{dr_1}{dr} 2isH_1^{(2)}(r_1) + \right.$$

$$\left. B_1 \frac{dr_2}{dr}(2s^2 - W^2)H_1^{(1)}(r_2) + B_2 \frac{dr_2}{dr}(2s^2 - W^2)H_1^{(2)}(r_2)\right],$$

$$u_{rF}^{(1)} = -C_2 \frac{dr_{11}}{dr} H_1^{(2)}(r_{11}) + D_2 \frac{dr_{21}}{dr} isH_1^{(2)}(r_{21}), \quad u_{zF}^{(1)} = -C_2 isH_0^{(2)}(r_{11}) + D_2(W_1^2 - s^2)H_0^{(2)}(r_{21}),$$

$$\sigma_{rrF}^{(1)} = \mu^{(1)}\left[C_2\left(-(1+\frac{\lambda^{(1)}}{2\mu^{(1)}})\left(\frac{dr_{11}}{dr}\right)^2 (H_0^{(2)}(r_{11}) - H_2^{(2)}(r_{11})) - \right.\right.$$

$$\left.\frac{\lambda^{(1)}}{\mu^{(1)}}\frac{dr_{11}}{dr} H_1^{(2)}(r_{11}) - \frac{\lambda^{(1)}}{\mu^{(1)}} s^2 H_0^{(2)}(r_{11})\right) + D_2\left(-(1+\frac{\lambda^{(1)}}{2\mu^{(1)}})\left(\frac{dr_{21}}{dr}\right)^2 is(H_0^{(2)}(r_{21}) - H_2^{(2)}(r_{21})) + \right.$$

$$\left.\left.\frac{\lambda^{(1)}}{\mu^{(1)}}\frac{1}{r}\frac{dr_{21}}{dr} isH_1^{(2)}(r_{21}) - \frac{\lambda^{(1)}}{\mu^{(1)}} is(W^2 - s^2)H_0^{(2)}(r_{21})\right)\right],$$

$$\sigma_{rzF}^{(1)} = \mu^{(2)}\left[C_2 \frac{dr_{11}}{dr} 2isH_1^{(2)}(r_{11}) + D_2 \frac{dr_{21}}{dr}(2s^2 - W_1^2)H_1^{(2)}(r_{21})\right].$$

Substituting the expressions in (18) into the Fourier transformation of the boundary (4), (11) and contact conditions (5) we obtain the following system of algebraic equations for the unknowns A_1, A_2, B_1, B_2, C_2 and D_2.

$$A_1\alpha_{1j} + A_2\alpha_{2j} + B_1\alpha_{3j} + B_2\alpha_{4j} + C_2\alpha_{5j} + D_2\alpha_{6j} = -P_0\delta_j^1, \quad j = 1,2,...,6. \tag{19}$$

Note that the explicit expressions of the coefficients α_{ij} ($i;j$ = 1,2,…,6) can easily be determined from the expressions in (18).

According to Eq. (19), the aforementioned unknown constants A_1, A_2, B_1, B_2, C_2 and D_2 can be presented as follows

$$A_1 = \frac{\det(\beta_{mj}^{(1)})}{\det(\alpha_{mj})}, \quad A_2 = \frac{\det(\beta_{mj}^{(2)})}{\det(\alpha_{mj})}, \quad B_1 = \frac{\det(\beta_{mj}^{(3)})}{\det(\alpha_{mj})}, \quad B_2 = \frac{\det(\beta_{mj}^{(4)})}{\det(\alpha_{mj})}, \quad C_2 = \frac{\det(\beta_{mj}^{(5)})}{\det(\alpha_{mj})}, \quad D_2 = \frac{\det(\beta_{mj}^{(6)})}{\det(\alpha_{mj})} \tag{20}$$

where the matrix $(\beta_{mj}^{(k)})$ is obtained from the matrix (α_{mj}) by replacing the $k-th$ column of the latter one with the column $(-P_0\delta_j^1)$.

Thus, we determine completely the Fourier transformation of the sought functions. The originals of these functions are determined from the inverse Fourier transformation (12).

4. Numerical results and discussions

In this section, first, we consider the algorithm for calculation of the integral in (12) and consider numerical examples illustrating its validation and after these considerations we present and discuss the numerical results on the critical velocity and on the response of the interface stresses to the oscillating moving load. All the numerical results which will be considered below are obtained in the following three cases.

$$\text{Case 1.}\quad E^{(1)}/E^{(2)} = 0.35\,,\quad \rho^{(1)}/\rho^{(2)} = 0.1\,,\quad \nu^{(1)} = \nu^{(2)} = 0.25\,. \tag{21}$$

$$\text{Case 2.}\quad E^{(1)}/E^{(2)} = 0.05\,,\quad \rho^{(1)}/\rho^{(2)} = 0.01\,,\quad \nu^{(1)} = \nu^{(2)} = 0.25\,. \tag{22}$$

$$\text{Case 3.}\quad E^{(1)}/E^{(2)} = 0.5\,,\quad \rho^{(1)}/\rho^{(2)} = 0.5\,,\quad \nu^{(1)} = \nu^{(2)} = 0.3\,. \tag{23}$$

Note that Case 1 and Case 2 are selected for comparison of the present results in particular cases with the corresponding ones obtained in the paper by Abdulkadirov (1981) (because these cases are also considered in that paper) and Case 3 is selected for comparison of the present results in particular cases with the corresponding ones obtained in the paper by Babich *et al*. (1986) in which this case is also considered.

4.1 The algorithm for calculation of the integrals (12)

The integrals in (12) are called the wavenumber integrals, because if we equate to zero the $\det(\alpha_{mj})$ in (20) and consider the Fourier transform parameter s as the wave number, then we obtain the dispersion equation for the corresponding longitudinal axisymmetric wave propagation. In the case under consideration, for construction of the dispersion curve it is necessary to consider not only the positive wavenumbers s, but also the negative wavenumbers s. In other words, the solution $W = W(s)$ to the equation $\det(\alpha_{mj}) = 0$ must be obtained for $s \in (-\infty, +\infty)$. It is evident that this solution is also the singular points of the integrated functions in (12), i.e., the integrated functions in (12) have singular points with respect to s and if the order of this singularity is equal to one, then the integrals have a meaning in Cauchy's principal value sense. However, in the cases where the order of the singularity is equal to two, then these cases cause resonance type behavior of the system under consideration. Namely, this situation complicates calculation of the integrals in (12). How to calculate these integrals is described and applied in the works by Tsang (1978), Jensen at al. (2011), Akbarov (2015), Akbarov and Ismailov (2016b) and others listed therein.

Thus, the algorithm which we use in the present investigation is based on Cauchy's well-known theorem, according to which, the contour $[-\infty, +\infty]$ is "deformed" into the contour C (Fig. 2) and the latter one is called the Sommerfeld contour in the complex plane $s = s_1 + is_2$ and in this way the real roots of the equation $\det(\alpha_{mj}) = 0$ are avoided. It should be noted that despite this avoidance, the values of the integrals calculated by the Sommerfeld contour algorithm have a jump in the near vicinity of the second order singular points and using this statement the aforementioned algorithm can be employed for determination of the critical values of a moving or oscillating moving load velocity. Such applications with respect to concrete problems, as examples, are made in the monograph by Akbarov (2015).

Hence, according to the foregoing discussions, the integrals in (12) can be presented as follows

$$\left\{\Phi^{(k)};\Psi^{(k)};u_z^{(k)};u_r^{(k)};\sigma_{nn}^{(k)};\sigma_{rz}^{(k)};\varepsilon_{nn}^{(k)};\varepsilon_{rz}^{(k)}\right\}(r,z) =$$
$$\frac{1}{2\pi}\int_C\left\{\Phi_F^{(k)}\Psi_F^{(k)};u_{zF}^{(k)};u_{rF}^{(k)};\sigma_{nnF}^{(k)};\ \sigma_{rzF}^{(k)};\varepsilon_{nnF}^{(k)};\varepsilon_{rzF}^{(k)}\right\}(r,s)e^{-isz}ds\,,\quad nn = rr;\theta\theta;zz\,. \tag{24}$$

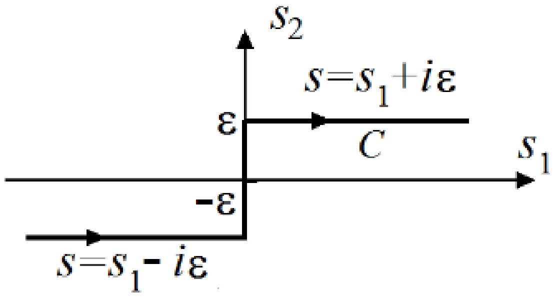

Fig. 2 The sketch of the Sommerfeld contour

Using the configuration of the contour C given in Fig. 2 the following relation for the integrals in (24) can be written.

$$\int_C f(s)e^{-isz}ds = \int_0^{+\infty}\left[f(s_1+i\varepsilon)+f(-s_1-i\varepsilon)\right]\times$$
$$\cos((s_1+i\varepsilon)z)ds_1 - i\int_0^{+\infty}\left[f(s_1+i\varepsilon)-f(-s_1-i\varepsilon)\right]\times\sin((s_1+i\varepsilon)z)ds_1 + i\int_{-\varepsilon}^{+\varepsilon} f(is_2)ds_2\,. \tag{25}$$

Supposing that $\varepsilon \ll 1$ we can neglect the last integral on the right side of the relation (25) and use the following expression for calculation of the integrals in (24).

$$\int_C f(s)e^{-isz}ds \approx \int_0^{+\infty}\left[f(s_1+i\varepsilon)+f(-s_1-i\varepsilon)\right]\cos((s_1+i\varepsilon)z)ds_1 -$$
$$i\int_0^{+\infty}\left[f(s_1+i\varepsilon)-f(-s_1-i\varepsilon)\right]\sin((s_1+i\varepsilon)z)ds_1\,. \tag{26}$$

Note that under calculation of the integrals in (26) the improper integral $\int_0^{+\infty}(\bullet)ds_1$ is replaced with the corresponding definite integral $\int_0^{S_1^*}(\bullet)ds_1$ and the values of S_1^* are defined from the corresponding convergence requirement. Moreover, under calculation of the integral $\int_0^{S_1^*}(\bullet)ds_1$, the interval $[0, S_1^*]$ is divided into a certain number (denote this number through N) of shorter intervals and within each of these shorter intervals the integrals are calculated by the use of the Gauss quadrature method with ten integration points. The values of the integrated functions at these integrated points are calculated through the solution of the system of algebraic equations in (19) and it is assumed that in each of the shorter intervals the sampling interval Δs_1 of the numerical integration must satisfy the relation $\Delta s_1 \ll \min\{\varepsilon, 1/z\}$. All these procedures are performed automatically in the PC by use of the corresponding programs constructed by the authors of the paper in MATLAB.

4.2 Testing of the calculation algorithm

We test the calculation algorithm with respect to Case 1 (21) for the frequency response of the normal stress

$$\sigma_{rr}(z) = \sigma_{rr}^{(1)}(R,z) = \sigma_{rr}^{(2)}(R,z) \tag{27}$$

i.e., the relation between the stress σ_{rr} (=$\sigma_{rr}(0)$) and dimensionless frequency Ω determined by the expression in (15) under $S_1^* = 9$, $\varepsilon = 0.01$, $h/R = 0.1$ and $c = 0.5$, where c is also determined by the expression in (15).

Thus, we consider the results illustrated in Figs. 3a and 3b which illustrate the convergence of the numerical results with respect to the number N. Note that for clarity of the illustrations, the results obtained for the cases where $N \leq 100$ (in the case where $N \geq 150$) are given in Fig. 3a (in Fig. 3b). It follows from these results and other ones which are not given here, that under $N \geq 200$ the numerical results obtained for various N coincide with each other with accuracy 10^{-8} -10^{-9}. Taking this statement into consideration, obtaining the numerical results given below are calculated under $N = 200$.

Now we consider the results given in Fig. 3c which illustrate the convergence of the numerical results with respect to S_1^* under $N = 200$. It follows from these results and other ones which are not given here, that in the cases where $S_1^* \geq 9$ the numerical results obtained for various S_1^* coincide with each other with accuracy 10^{-8} -10^{-9}. Taking this situation into consideration, the results discussed below are obtained in the case $S_1^* = 9$.

Finally, we consider the numerical results given in Fig. 3d which illustrate the convergence of the employed algorithm with respect to the parameter ε. These results show that it is sufficient to take $\varepsilon = 0.01$ in order to avoid the real roots of the corresponding dispersion equation and to obtain guaranteed numerical results.

Thus, according to the foregoing results and other similar ones which are not illustrated here, under obtaining all the numerical results which will be discussed below, we assume that $N = 200$, $S_1^* = 9$ and $\varepsilon = 0.01$.

4.3 Numerical results related to the critical velocity

According to the data given in (21), (22) and (23), it can be written that

$$\frac{c_2^{(1)}}{c_2^{(2)}} = 3.5 \quad \text{in Case 1,} \quad \frac{c_2^{(1)}}{c_2^{(2)}} = 5 \quad \text{in Case 2 and} \quad \frac{c_2^{(1)}}{c_2^{(2)}} = 1.0 \quad \text{in Case 3.} \tag{28}$$

It follows from the relations in (28) that the shear wave propagation velocity in the material of the hollow cylinder in Case 1 and Case 2 is less than, while in Case 3 it is equal to, that of the surrounding elastic medium. We recall that the critical velocity of the moving load appears in the cases where the modulus of elasticity of the hollow cylinder is greater than that of the surrounding elastic medium. Moreover, we recall that in the present investigation it is assumed that the velocity of the moving load is subsonic, i.e., it is assumed that $c = V/c_2^{(2)} < 1.0$.

Thus, we consider the numerical results related to the critical velocity and to the influence of the problem parameters on this velocity. First, we note the approach where the critical velocity is determined. This approach is based on construction of the graphs between the sought quantities and load moving velocity (for instance, between σ_{rr} (=$\sigma_{rr}(0)$) and c).

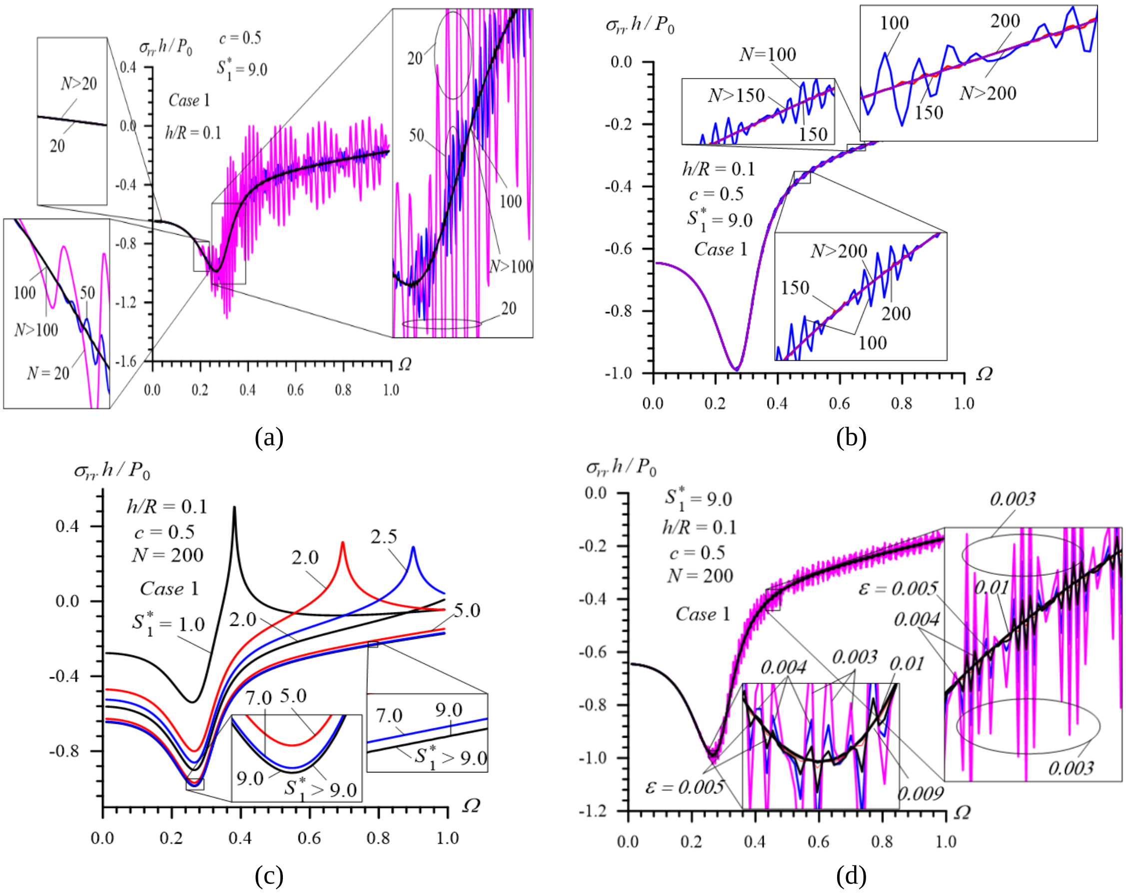

Fig. 3 Convergence of the numerical results with respect to the number N (a; b), to the integration interval S_1^* (c) and to the parameter ε(d)

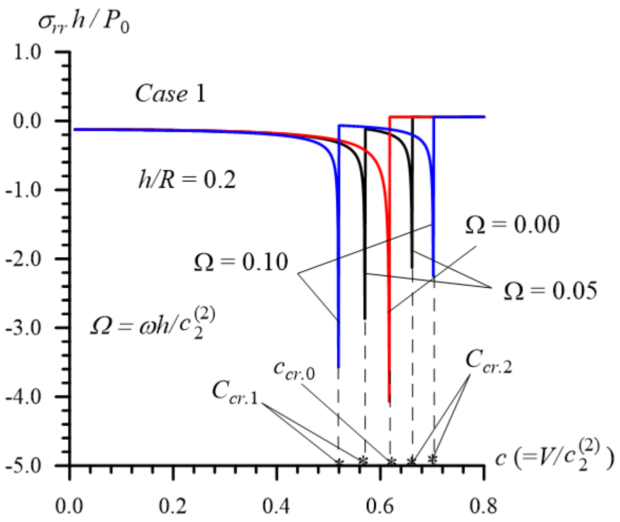

Fig. 4. Example results for determination of the critical velocities

Table 1 Dimensionless critical velocities in Case 1: Numerator (denominator) shows the numbers of the set $C_{cr.1}$ (the set $C_{cr.2}$)

Ω	h/R 0.5	0.2	0.1	0.02
0.0	0.935 (0.935 Abdulkadirov 1981)	0.864	0.843	0.831
0.01	0.933 / 0.936	0.858; / 0.868;0.924	0.836 / 0.848;0.922	0.824 / 0.838;0.920
0.05	0.922;0.931 / 0.946	0.836 / 0.888;0.916;0.928	0.810 / 0.872;0.926	0.796 / 0.862;0.926;0.958
0.1	0.907;0.925 / 0.947	0.806; / 0.910;0.936	0.774 / 0.896;0.908;0.932	0.754 / 0.890;0.908;0.932
0.2	0.873;0.914 / 0.958	0.734 / 0.900;0.950	0.676 / 0.898;0.938;0.948	– / 0.896;0.934;0.946
0.3	0.835;0.903 / 0.970	0.635 / 0.889;0.956	– / 0.887;0.964;0.971	– / 0.885; 0.963
0.4	0.790;0.892 / 0.979	– / 0.878;0.976	– / 0.876;0.964	– / 0.874;0.963
0.5	0.739;0.880;0.833 / 0.980	– / 0.866;0.988	0.864 / 0.988	– / 0.864
0.6	0.681;0.870; 0.717 / 0.969	0.855 / 0.967	0.853 / 0.967	– / 0.852;0.967
0.7	0.609;0.858 / 0.958	0.844 / 0.956	0.842 / 0.956	– / 0.840;0.936
0.8	0.847 / 0.947	0.825 / 0.869	0.831 / 0.945	0.830 / 0.945
1.0	0.825 / 0.924	0.810 / 0.922	0.808 / 0.898	0.808 / 0.922

If in a certain value of c the absolute value of σ_{rr} has a jump, such as illustrated in Fig. 4, then this value of c is selected as a critical velocity. As an example, this procedure is illustrated in Fig. 4 with respect to Case 1 under various values of the oscillation frequency Ω of the moving load under h/R = 0.2. The numerical results given in Fig. 4 and many others which are not given here show that in the case where $\Omega = 0$ the moving load has only one critical velocity (denote it by $c_{cr.0}$). However, in the cases where $\Omega > 0$ the moving load has several critical velocities, some of which are greater than $c_{cr.0}$ (the set of such critical velocities we denote through $C_{cr.2}$ in Fig. 4), but the other ones are less than $c_{cr.0}$ (the set of such critical velocities we denote through $C_{cr.1}$ in Fig. 4).

Thus, we analyze the obtained critical velocities which are determined by employing the foregoing approach and according to this analysis we determine the character of the influence of the problem parameters such as Ω and h/R on these critical velocities for the pairs of materials determined through the relations (21), (22) and (23). Under the discussion below, as in Fig. 4, through $c_{cr.0}$ we will denote the critical velocity obtained under Ω = 0, however, through $C_{cr.1}$ (through $C_{cr.2}$) we will denote the set of critical velocities obtained in the cases where $\Omega > 0$ and which are less (greater) than $c_{cr.0}$.

Consider Tables 1, 2 and 3 which show the values of the aforementioned critical velocities in Case 1, Case 2 and Case 3, respectively. Note that in Case 1 and Case 2 under h/R = 0.5 and

Table 2 Dimensionless critical velocities in Case 2: Numerator (denominator) shows the numbers of the set $C_{cr.1}$ (the set $C_{cr.2}$)

Ω	h/R				
	0.5	0.2	0.1	0.05	0.02
0	0.826 (0.826 by Abdulkadirov (1981))	0.617	0.529	0.478	0.471
0.01	$\frac{0.820}{0.830; 0.922; 0.962}$	$\frac{0.608}{0.626}$	$\frac{0.516}{0.540}$	$\frac{0.473}{0.502}$	$\frac{0.454}{0.488}$
0.05	$\frac{0.804}{0.846; 0.916; 0.928}$	$\frac{0.570}{0.660}$	$\frac{0.460}{0.588}$	$\frac{0.404}{0.558}$	$\frac{0.374}{0.546}$
0.1	$\frac{0.780}{0.866; 0.910; 0.932}$	$\frac{0.518}{0.702}$	$\frac{0.382}{0.640}$	$\frac{-}{0.622}$	$\frac{-}{0.608}$
0.2	$\frac{0.732}{0.902; 0.944}$	$\frac{0.400}{0.776}$	$\frac{-}{0.734}$	$\frac{-}{0.718}$	$\frac{-}{0.714}$
0.3	$\frac{0.681}{0.888; 0.935; 0.955}$	$\frac{0.249}{0.635}$	$\frac{-}{0.812}$	$\frac{-}{0.802}$	$\frac{-}{0.799}$
0.4	$\frac{0.624}{0.877; 0.919; 0.962}$	$\frac{-}{0.869}$	$\frac{-}{0.877}$	$\frac{-}{0.871}$	$\frac{-}{0.869}$
0.5	$\frac{0.562}{0.866; 0.978}$	$\frac{-}{0.858}$	$\frac{-}{0.856}$	$\frac{-}{0.856}$	$\frac{-}{0.856}$
0.6	$\frac{0.495}{0.855; 0.897; 0.988}$	$\frac{-}{0.847}$	$\frac{-}{0.846}$	$\frac{-}{0.845}$	$\frac{-}{0.845}$
0.7	$\frac{0.420}{0.844; 0.866}$	$\frac{-}{0.836}$	$\frac{-}{0.834}$	$\frac{-}{0.834}$	$\frac{-}{0.834}$
0.8	$\frac{0.730}{0.833; 0.875}$	$\frac{-}{0.825}$	$\frac{-}{0.823}$	$\frac{-}{0.823}$	$\frac{-}{0.823}$
1.0	$\frac{0.810}{0.852}$	$\frac{-}{0.802}$	$\frac{-}{0.802}$	$\frac{-}{0.800}$	$\frac{-}{0.800}$

$\Omega = 0.0$ the critical velocities are also calculated in the paper by Abdulkadirov (1981). Therefore, in Tables 1 and 2 the corresponding results obtained in the paper by Abdulkadirov (1981) are also given for comparison with the present ones obtained in related particular cases. It follows from this comparison that the present results coincide completely with those obtained in the paper by Abdulkadirov (1981). Moreover, the numerical results in Case 3 must be approaching to corresponding ones obtained in the paper by Babich *et al*. (1986) with decreasing of the ratio h/R. This prediction is proven with data obtained under $\Omega = 0.0$ and given in Table 3. Consequently, the foregoing comparison shows that the numerical results obtained in the present paper, in particular cases, coincide with the corresponding ones obtained earlier by other researchers. This situation gives certain guarantees on the reliability of the solution approach and PC algorithm and programs used in the present paper.

Thus, we turn to the analysis of the data given in Tables 1, 2 and 3 and note that in these tables the values of the critical velocities which enter into the set $C_{cr.1}$ (the set $C_{cr.2}$) are obtained for the cases where $\Omega > 0$ and given in the numerator (denominator). Moreover, we note that in these tables, the symbol “-” denotes that in the corresponding case there is no critical velocity. It follows

Table 3 Dimensionless critical velocities in Case 3: Numerator (denominator) shows the numbers of the set $C_{cr.1}$ (the set $C_{cr.2}$)

Ω	h/R 0.5	0.2	0.1	0.05	0.02
0	0.944	0.874	0.854	0.847	0.843 0.839 (by Babich *et al.* (1986))
0.01	0.937 / 0.941;0.945	0.868 / 0.879	0.847 / 0.861	0.839 / 0.854	0.835 / 0.850
0.05	0.925;0.937 / 0.951	0.844 / 0.900	0.816;0.832 / 0.885	0.803 / 0.879	0.794 / 0.877
0.1	0.909;0.931 / 0.953	0.808 / 0.922	0.824 / 0.911	– / 0.906	– / 0.904
0.2	0.871;0.920 / 0.961	– / 0.907	0.818 / 0.951	– / 0.948	– / 0.904;0.947
0.3	0.821;0.909 / –	– / 0.896	0.808 / 0.894	– / 0.894;0.967	– / 0.893;0.960
0.4	0.898 / –	– / 0.885	– / 0.883	– / 0.882;0.971	– / 0.882;0.971
0.5	0.886 / –	– / 0.874	– / 0.872	– / 0.871;0.987	– / 0.871;0.982
0.6	0.875 / –	0.863 / –	– / 0.861	– / 0.860	– / 0.860
0.7	0.864 / –	0.852 / –	0.850 / –	– / 0.849	– / 0.849
0.8	0.853 / –	0.841 / –	0.839 / –	0.838 / –	0.838 / –
1.0	0.831 / –	0.818 / –	0.817 / –	0.816 / –	0.816 / –

from the tables that the sets $C_{cr.1}$ and $C_{cr.2}$, may contain one, two or three numbers for each selected value of the frequency Ω.

We introduce the notation $c_{cr.11}$, $c_{cr.12}$ and $c_{cr.13}$ ($c_{cr.21}$, $c_{cr.22}$ and $c_{cr.23}$) for the numbers of the set $C_{cr.1}$($C_{cr.2}$) for which the relation $c_{cr.11} < c_{cr.12} < c_{cr.13} < c_{cr.0} < c_{cr.21} < c_{cr.22} < c_{cr.23}$ takes place. It follows from the tables that for each fixed case some of the critical velocities from the sets $C_{cr.1}$ and $C_{cr.2}$ exist and sometimes these velocities may disappear.

Thus, it follows from the analyses of these tables that, in general, before a certain value of Ω, the values of $c_{cr.11}$, $c_{cr.12}$ and $c_{cr.13}$ decrease with Ω. At the same time, it follows from the tables that before a certain value of Ω the values of $c_{cr.21}$, $c_{cr.22}$ and $c_{cr.23}$ increase. However, after the mentioned "certain value" of Ω, the value $c_{cr.1}$ or all the numbers of the set $C_{cr.1}$ or some of them, can disappear. Thus, if $c_{cr.11}$ disappears only, then $c_{cr.12}$ becomes the minimum of the set $C_{cr.1}$. In a similar manner, after the aforementioned "certain value" of Ω the values of $c_{cr.21}$ decrease with Ω. It follows from Tables 1 and 2 that in Case 1 and Case 2 there are many cases under which all the critical velocities which are less than $c_{cr.0}$ disappear. However, in Case 1 and Case 2 for the considered range change of the problem parameters the critical velocity from the set $C_{cr.2}$ exists under each selected value of the problem parameters. At the same time, Table 3 shows that in Case

Table 4 The values of the “weak” critical velocities

			h / *R*		
Ω	0.5	0.2	0.1	0.05	0.02
			Case 1		
0.2	-	-	-	0.626	0.612
0.3	-		0.502	0.495	0.448
0.4	-	0.460	0.328	-	-
0.8	0.511	-	-	-	-
			Case 2		
0.1	-	-	-	0.266	0.194
0.3	-	-	0.496	-	-
0.33	-	0.177	-	-	-
0.38	-	0.119	-	-	-
			Case 3		
0.1	-	-	0.754	0.737	0.731
0.2	-	0.697	0.682	0.636	0.614
0.3	-	0.604	0.590	0.549	0.555
0.4	0.764	0.516	0.572	-	-
0.5	0.706	0.418	-	-	-
0.6	0.641	0.310	-	-	-
0.7	0.591	-	-	-	-
0.8	0.522	-	-	-	-
1.0	0.406	-	-	-	-

3 after a certain value of Ω, not only can all the critical velocities which are greater than $c_{cr.0}$ disappear, but there is also the case under which all the critical velocities from the set $C_{cr.1}$ can disappear.

The numerical results given in the foregoing tables also show that the critical velocities decrease with the ratio h / R and with decreasing of this ratio the “certain value” of Ω, after which the critical velocities from the set $C_{cr.1}$ disappear completely, decreases. For instance, in Case 2 for $h / R = 0.2$ under $\Omega \geq 0.4$, for $h / R = 0.1$ under $\Omega \geq 0.2$ and for $h / R \leq 0.05$ under $\Omega \geq 0.1$ the critical velocities which are less than $c_{cr.0}$ disappear completely. A similar relation can also be formulated for the data given in Tables 1 and 3 for Case 1 and Case 3, respectively.

Note that this statement in the qualitative sense agrees with the corresponding ones obtained in the papers by Dieterman and Metrikine (1997), Akbarov and Salmanova (2009) and other ones which are detailed and listed in the monograph by Akbarov (2015).

Thus, according to the foregoing discussions and according to the numerical results given in Tables 1, 2 and 3 some general conclusions, which are given in the next section, can be made.

Note that more concrete special conclusions can easily be made from the tables for each selected pair of materials, the examples for which are done above. With this we restrict ourselves to the analysis of the numerical results related to the critical velocity and to the influence of the problem parameters, such as the mechanical properties of the selected pairs of materials,

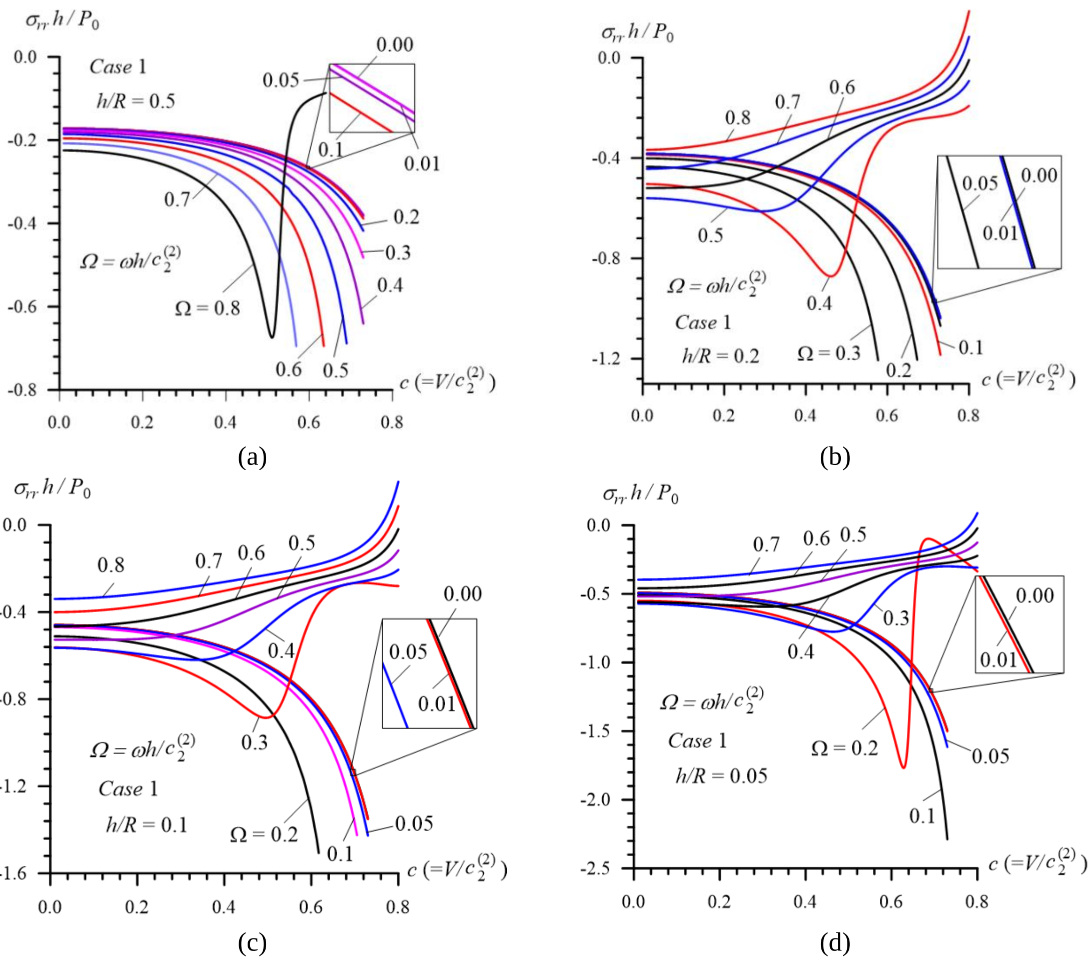

Fig. 5 Graphs of the dependence between the interface normal stress σ_{rr} and load moving velocity c for various frequency Ω of the oscillation of this load under $h / R = 0.5$ (a), 0.2 (b), 0.1 (c) and 0.05 (d) in Case 1

oscillation frequency of the moving load and ratio of the cylinder's thickness/radius. In the authors' opinion, the main conclusion of the foregoing analysis is that an increase of the oscillation of the moving load and a decreasing of the thickness of the hollow cylinder under constant external radius of this cylinder can cause the critical velocity of the oscillating moving ring load acting in the interior of the cylinder surrounded with an elastic medium, to decrease significantly.

4.3 Numerical results related to the stress responses

First, we analyze the graphs of the dependence between σ_{rr} ($=\sigma_{rr}(0)$) (27) and load moving velocity c constructed for various values of the frequency Ω and of the ratio h / R. The graphs obtained for Case 1, Case 2 and Case 3 are given in Figs. 5, 6 and 7 respectively and the graphs in these figures grouped by letters a, b, c and d correspond to the cases where $h / R = 0.5$, 0.2, 0.1 and 0.05, respectively. Note that in the cases where the critical velocity related to the set $C_{cr.1}$ exists, the

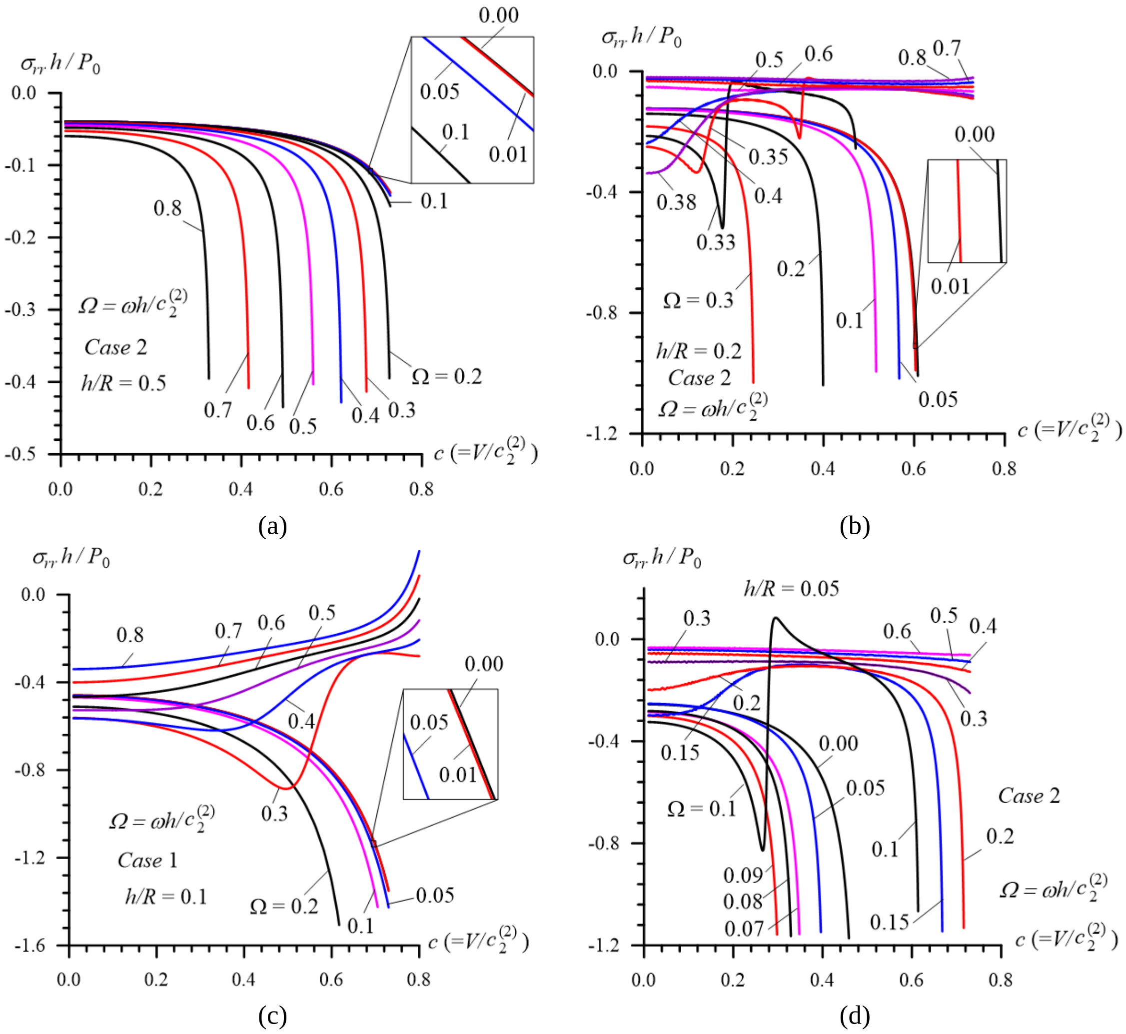

Fig. 6 Graphs indicated in Fig. 5 caption and constructed in Case 2

corresponding graphs are constructed before a certain value of c which is less than the mentioned critical velocity. However, in the cases where the critical velocity related to the set $C_{cr.1}$ does not exist, the graphs are constructed for the considered change range of c which is indicated in the figures. Namely, in these latter cases, in certain values of the frequency Ω, the dependence between σ_{rr} and c has a clearly identified maximum in the absolute value sense for a certain value of c. For instance, such maximums in Case 1 appear under $\Omega = 0.8$ for $h / R = 0.5$ (Fig. 5a), under $\Omega = 0.4$ and 0.5 for $h / R = 0.2$ (Fig. 5b), under $\Omega = 0.3$, 0.4 and 0.5 for $h / R = 0.1$ (Fig. 5c) and under $\Omega = 0.2$, 0.3 and 0.4 for $h / R = 0.05$ (Fig. 5d). Such maximums also appear in Case 2 and Case 3. For instance, in Case 3 these maximums appear in the following values of the frequency Ω: Under all considered Ω for $h / R = 0.5$ (Fig. 7a), under $\Omega = 0.1$, 0.2, 0.3, 0.4 and 0.5 for $h / R = 0.2$ (Fig. 7b), under $\Omega = 0.1$, 0.2, 0.3 and 0.4 for $h / R = 0.1$ (Fig. 7c) and under $\Omega = 0.1$, 0.2 and 0.3 for $h / R = 0.05$ (Fig. 7d). However, in the cases where Ω is greater than a certain value of that, the absolute values of the stress σ_{rr} decrease with the moving velocity of the ring load.

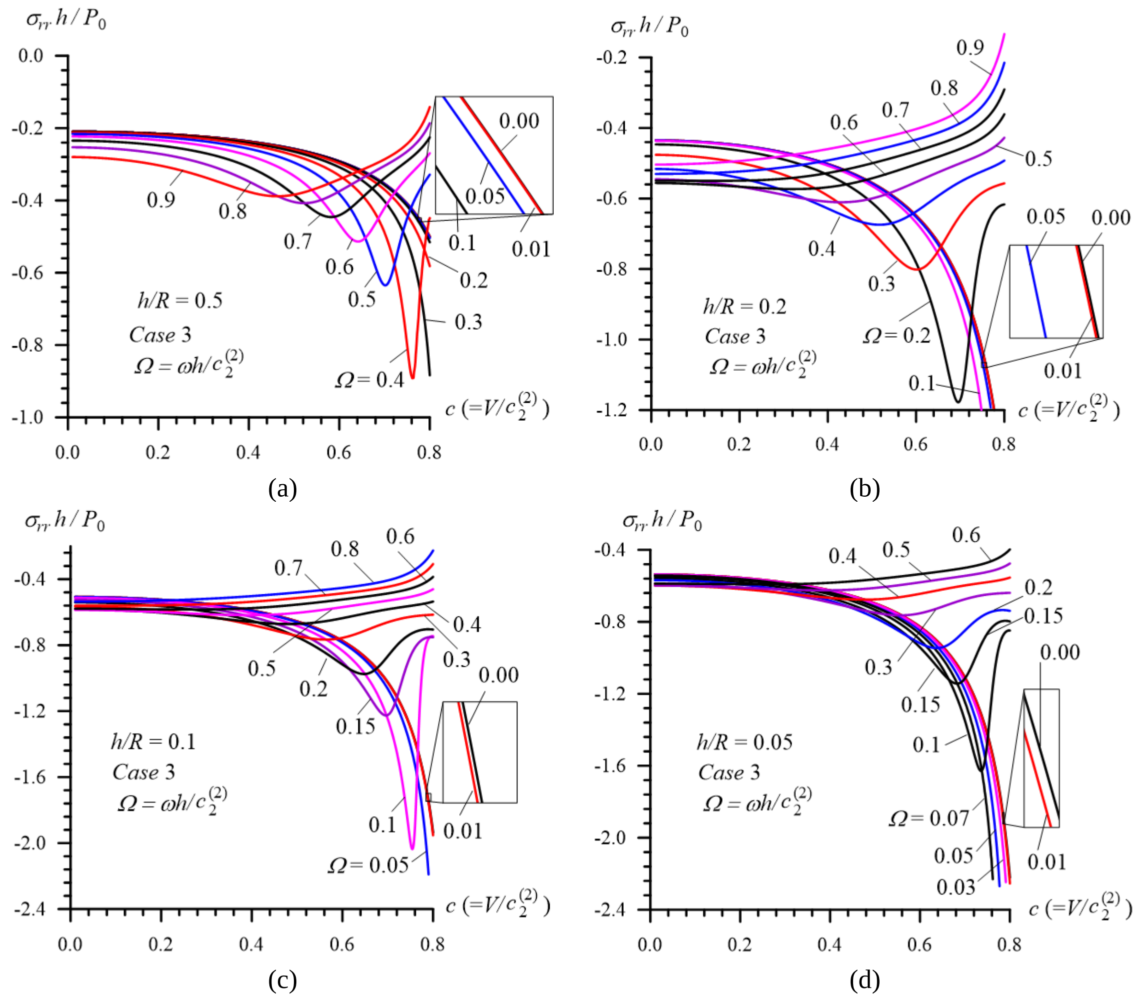

Fig. 7 Graphs indicated in Fig. 5 caption and constructed in Case 3

Note that in some references (for instance, see Hasheminejad and Komeili (2009), Shi and Selvadurai (2016) and others listed therein), the moving velocities corresponding to the foregoing maximums are also called the critical velocities, although in these cases resonance type accidents do not take place. Taking this statement into consideration we can also define the aforementioned values of the load moving velocity as the critical velocities and call them "weak" critical velocities in order to distinguish them from those determined in the previous sub-section. Note that as follows from the numerical results given in Figs. 5, 6 and 7 and other ones which are not given here, in many cases the "weak" critical velocities may also be dangerous ones for systems consisting of the hollow cylinder and surrounding elastic medium.

Table 4 shows the values of the aforementioned "weak" critical velocities obtained in Case 1, Case 2 and Case 3 from which it follows that the values of these velocities decrease monotonically with the oscillation frequency of the moving load Ω and with the ratio h / R. As in the previous tables, in Table 4 the symbol "-" means that in the corresponding case there is no "weak" critical velocity.

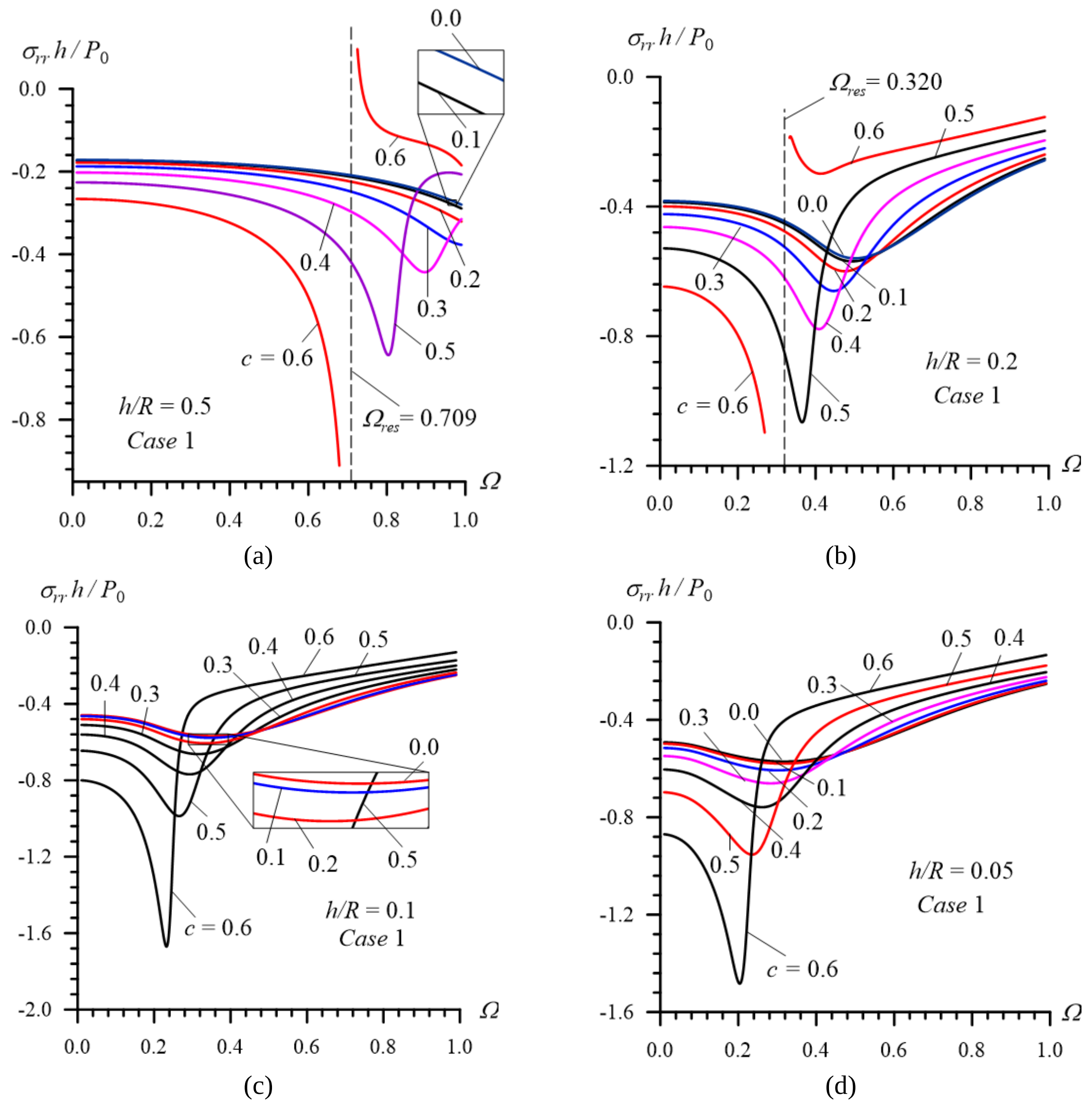

Fig. 8 Frequency response of the interface normal stress σ_{rr} obtained for various values of the load moving velocity under $h / R = 0.5$ (a), 0.2 (b), 0.1 (c) and 0.05 (d) in Case 1

Now we consider the results related to the frequency response of the interface stress σ_{rr} ($=\sigma_{rr}(0)$) which are obtained for various moving velocities of the ring load and for various ratios h / R. The graphs of these responses are given in Figs. 8 (for Case 1), 9 (for Case 2) and 10 (for Case 3) and in these figures the results grouped by letters a, b, c and d relate to the cases where h / R =0.5, 0.2, 0.1 and 0.05, respectively. Note that under construction of these graphs it is assumed that $0\leq c \leq 0.6$.

It follows from Figs. 8, 9 and 10 that in all the cases under consideration (except the case where h / R =0.5 and $0\leq c \leq 0.3$ in Case 1 and Case 2 and $0\leq c \leq 0.1$ in Case 3 under which the absolute values of the stress increase with Ω in the considered change range) the frequency responses have non-monotonic character, i.e., there are such values of Ω (denote this value of Ω by Ω^*) before

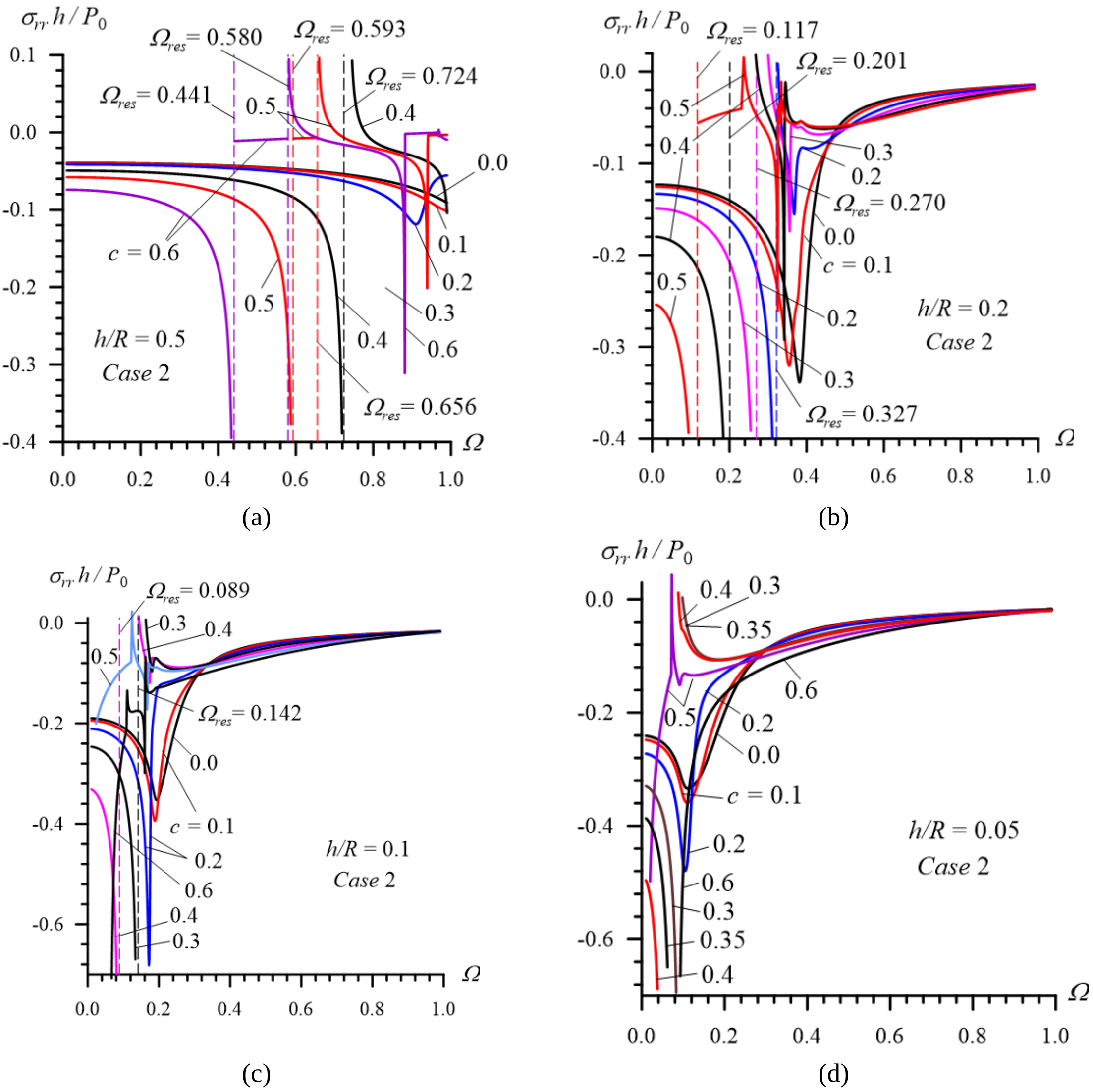

Fig. 9 Graphs indicated in Fig. 8 caption and constructed in Case 2

which the absolute value of the stress σ_{rr} becomes maximum and this maximum increases with the moving velocity of the ring load. At the same time, it follows from the results that the values of Ω^* decrease monotonically with c. Moreover, Figs. 8a, 8b, 9a, 9b, 9c and 9d show that there may be cases where an increase in the values of c leads to resonance cases. Such resonance cases and the corresponding resonance frequencies are indicated in these figures (except Fig. 9d).

The above-noted resonances can be estimated as a parametric resonance and as a parameter it can be taken as the load moving velocity. Consequently, under oscillating moving load action of the ring load, resonance type accidents appear not only under critical moving velocities of this load but also under the foregoing type of parametric resonances. Analyses of the foregoing results also show that the absolute maximum values of the stress under consideration increase with decreasing of the ratio h / R. Moreover, comparison of the results obtained for Case 1, Case 2 and Case 3 with

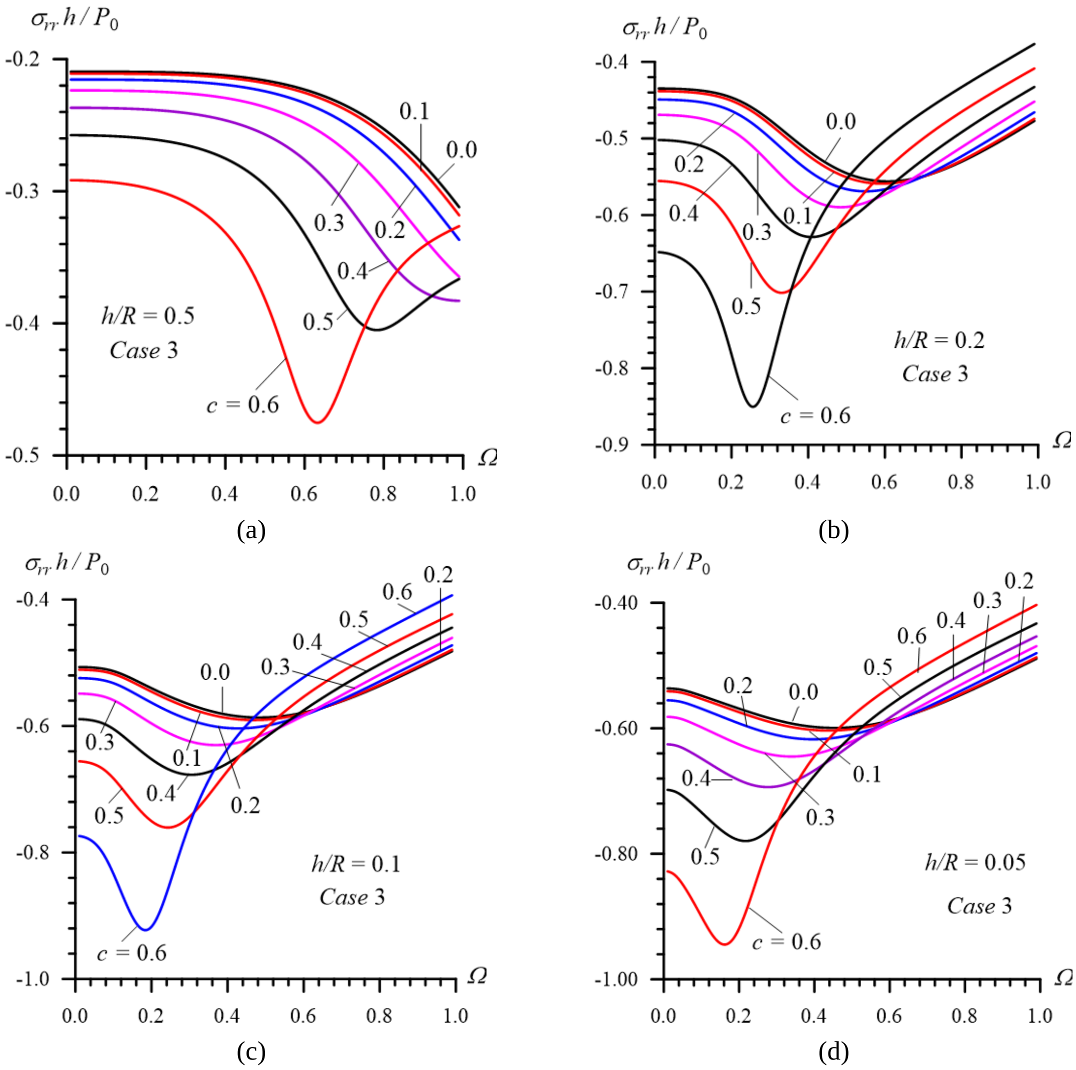

Fig. 10 Graphs indicated in Fig. 8 caption and constructed in Case 3

each other shows that the responses of the interface normal stress to the moving velocity of the ring load and its vibration depend not only on the values of this velocity and frequency, but also depend significantly on the ratio of the mechanical properties of the selected pairs of materials, as indicated in (21)-(23) and (28) for the hollow cylinder and surrounding elastic medium. At the same time, the latter dependence has not only quantitative, but also qualitative character.

Consider the numerical results related to the distribution of the normal stress σ_{rr}(z) (27) and shear stress

$$\sigma_{rz}(z) = \sigma_{rz}^{(1)}(R,z) = \sigma_{rz}^{(2)}(R,z)\,, \tag{29}$$

with respect to z/h. For this purpose we select Case 3 and consider the graphs given in Figs. 11 (for the normal stress σ_{rr}) and 12 (for the shear stress σ_{rz}) which illustrate these distributions under

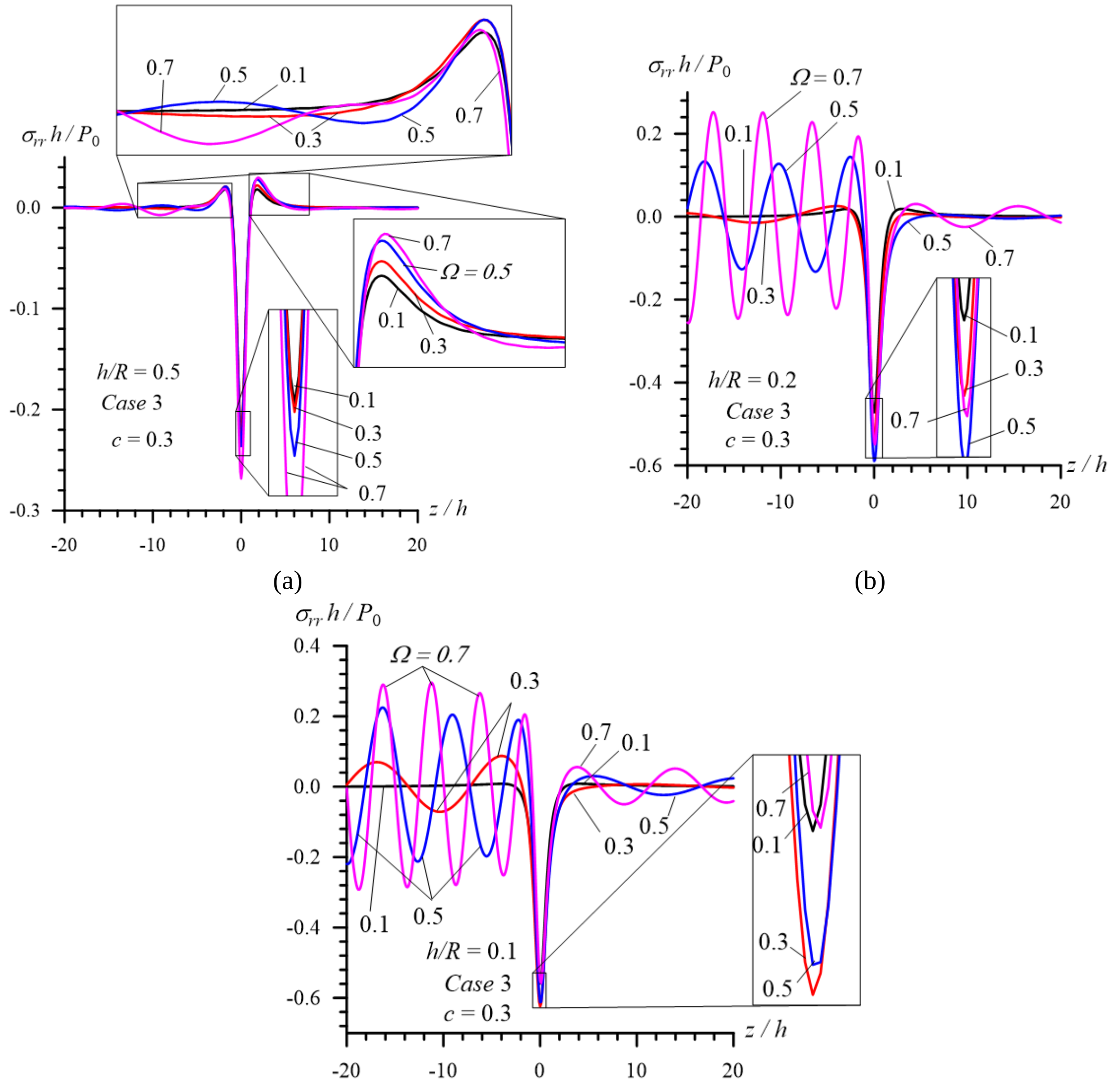

Fig. 11 Distribution of the interface normal stress σ_{rr} with respect to the axial coordinate z / h obtained for various oscillation frequencies Ω of the moving load in the case where the load moving velocity is $c = 0.3$ under $h / R = 0.5$ (a), 0.2 (b) and 0.1 (c) in Case 3

$c = 0.3$ for various values of the dimensionless frequency Ω. In these figures, the graphs grouped by letters a, b and c correspond to the cases where $h / R = 0.5$, 0.2 and 0.1, respectively. Note that the corresponding distributions related to the case where $c = 0.5$ are given in Figs. 13 (for the normal stress σ_{rr}) and 14 (for the shear stress σ_{rz}) and in these figures the graphs grouped by letters a and b relate to the cases where $h / R = 0.5$ and 0.2, respectively.

Thus, analyze the foregoing distribution and first of all note that in the case where $\Omega = 0$ the distribution of the stress $\sigma_{rr}(\sigma_{rz})$ is symmetric (asymmetric) with respect to the point $z / h = 0$. This symmetry and asymmetry for the stresses and other quantities of the problem under consideration

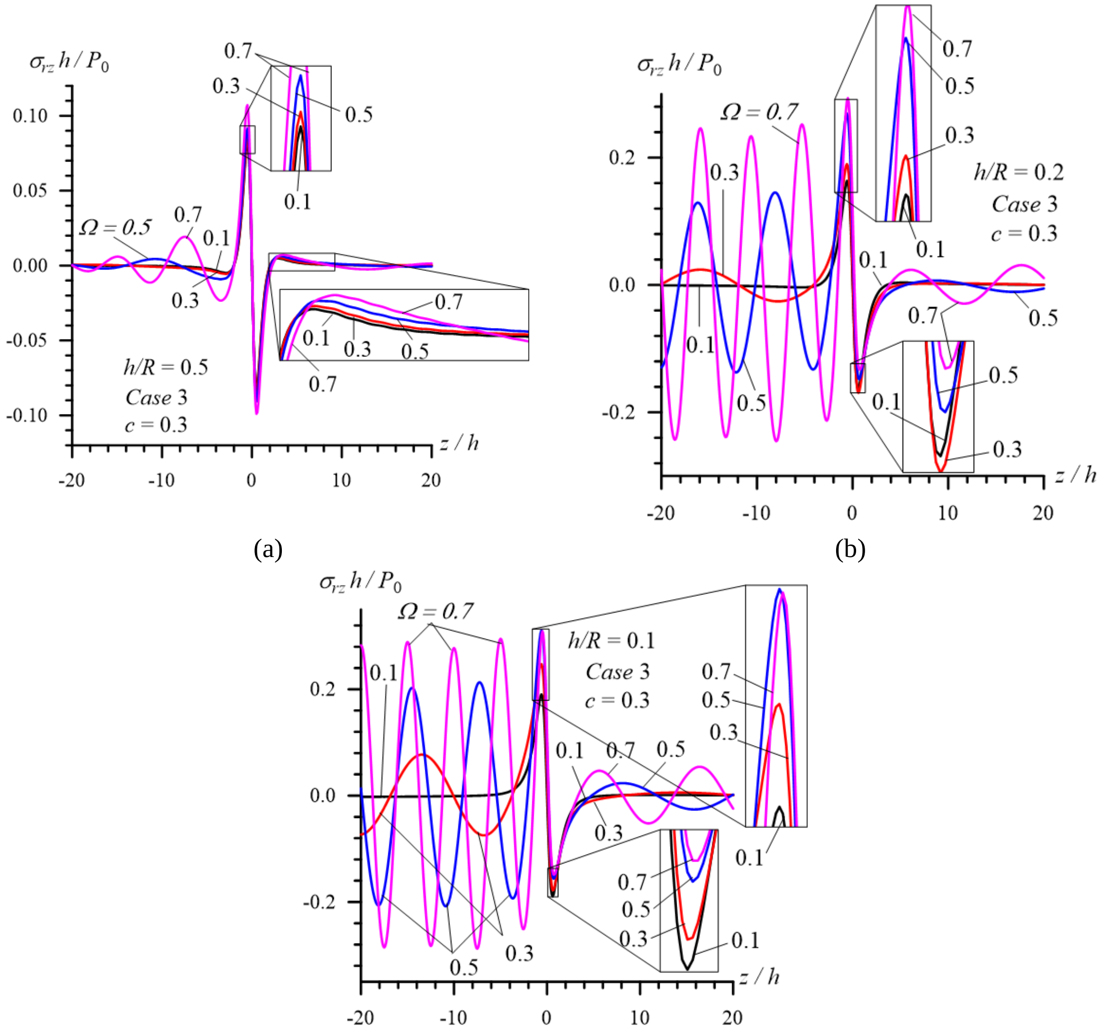

(c)

Fig. 12 Distribution indicated in Fig. 9 for the interface shear stress σ_{rz}

follow from the mechanical consideration, from the expressions of the equations given in (14) and from direct calculation of the corresponding distribution. However, in the case where $\Omega > 0$, as shown in Figs. 11-14, the aforementioned symmetry and asymmetry are violated and this violation increases with increasing of the frequency Ω and of the load moving velocity c. This is because the violation is caused by the term $-2s\Omega c$ of the expression for W^2 (15) which enters into the equation (14) and the magnitude of this term increases with increasing of Ω and c.

It follows from Figs. 11 and 13 that the normal stress σ_{rr} has its absolute maximum value at point $z / h = 0$ and dependence between this maximum and Ω are monotonic in the case where $h / R = 0.5$ and are non-monotonic in the cases where $h / R = 0.2$ and 0.1. Moreover, it follows from Figs. 11 and 13 that for relatively thick cylinders (for instance, for $h / R = 0.5$) attenuation of the normal stress with respect to $|z / h|$ takes place more rapidly than for relatively thin cylinders (for instance, for $h / R = 0.2$ and 0.1). Moreover, the results show that in the cases

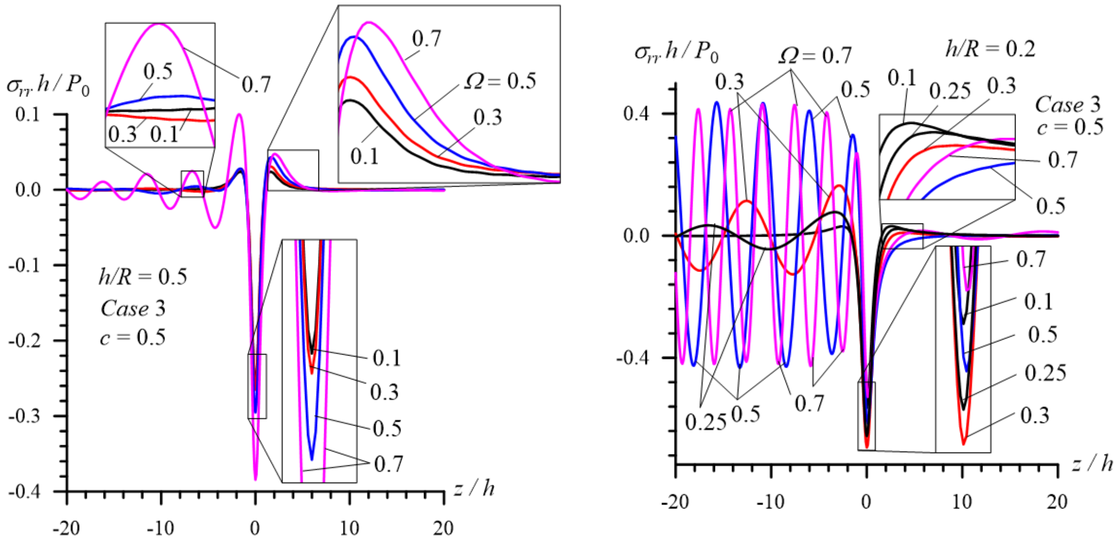

(a) (b)

Fig. 13 Distribution indicated in Fig. 9 and obtained for $c = 0.5$ under $h / R = 0.5$ (a) and 0.2 (b)

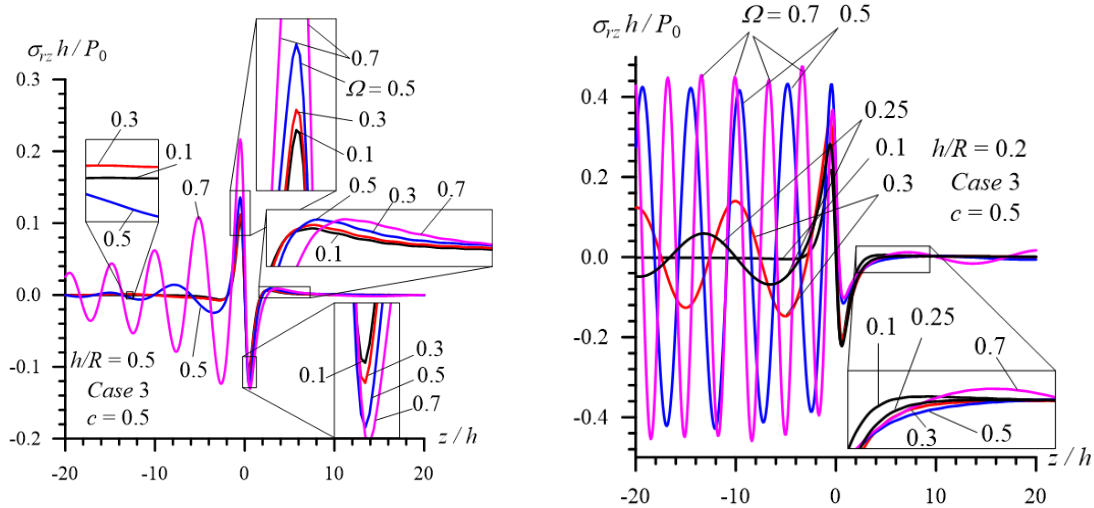

(a) (b)

Fig. 14 Distribution indicated in Fig. 10 and obtained for $c = 0.5$ under $h / R = 0.5$ (a) and 0.2 (b)

where h / R = 0.2 and 0.1, for behind and ahead of the moving load, non-attenuated periodic distributions appear and the amplitude of the behind distribution is greater than the corresponding one of the ahead distribution. At the same time, the amplitude (the period) of these distributions increases (decreases) with Ω and with c.

Note that in the qualitative sense the foregoing results relate also to the distribution of the shear stress σ_{rz} and are given in Figs. 12 and 14. However, this stress has its absolute maximum at a point which is behind the moving load.

4. Conclusions

Thus, in the present paper the axisymmetric problem on the dynamics of the oscillating moving ring load acting on the interior of the hollow cylinder surrounded by an elastic medium is investigated. The investigations are made with employing the exact equations and relations of linear elastodynamics. The focus is on the influence of the oscillation of the moving load on the values of the critical velocities. At the same time, the influence of the oscillation of the moving load on the dependence between the interface stress and moving load velocity, as well as the influence of the moving load velocity on the frequency response of the mentioned stress are also studied. Moreover, the distribution of the interface normal and shear interface stresses with respect to the axial coordinate is also detailed in the present study.

Thus, according to the discussions and the numerical results, the following general conclusions with respect to the critical velocities can be made:

- in the case where the moving load acting in the interior of the hollow cylinder does not have any oscillation, there is only one critical velocity of this load and this velocity decreases with decreasing of the ratio h / R;
- in the case where the moving load has oscillation, many critical velocities can appear, some of which are greater and others which are less than that obtained in the case where the oscillation of the load is absent;
- appearance and disappearance of the critical velocities for relatively great values of the oscillation frequency depend also on the selected pairs of materials of the hollow cylinder and surrounding elastic medium and on the ratio h / R;
- before a "certain frequency" of the oscillation, the minimum critical velocity which appears for relatively small values of the frequency and are less (greater) than $c_{cr.0}$, decreases (increases) with the frequency Ω and after this frequency the minimum critical velocities can disappear;
- all kinds of critical velocities decrease with decreasing of the ratio h / R;
- comparison of the critical velocities given in Tables 1, 2 and 3 allows us to formulate the following relation: In general, the critical velocities obtained in Case 2 are less than the corresponding ones obtained in Case 1 and the latter ones are less than the corresponding ones obtained in Case 3;
- it follows from the foregoing conclusion and from the data given in (21), (22) and (23) that despite the fact that the critical velocities of the moving load appear only in the cases where the modulus of elasticity of the cylinder material is greater than that of the surrounding elastic material, the values of the critical velocity depend not only on the ratio of these moduli but also on the ratio of the densities and on the Poisson coefficients of the selected pairs of materials;
- under studying the dependencies between the interface stress and load moving velocity it is established that under certain values of the load frequency, the so-called "weak" critical velocity can appear for which the absolute value of the stress becomes maximum.

The following conclusions can also be made for the response of the interface normal stress, from which the adhesion strength of the bi-material elastic system under consideration depends significantly on the moving velocity of the load and its oscillation frequency:

- in the cases where there exists the critical velocity $c_{cr.11}$ the absolute values of the stress increase monotonically with the moving velocity c ($< c_{cr.11}$) of the load;
- in the cases where the critical velocity $c_{cr.11}$ does not exist, then depending on the values of Ω two types of response of the stress to the moving velocity may appear: In the one which relates

to relatively small values of Ω, the dependence between the stress and velocity has non-monotonic character, but in the other one, which relates to relatively great values of Ω, the absolute values of the stress decrease monotonically with the moving load velocity;

- the frequency response of the stress depends not only on the moving load velocity, but also depends significantly on the ratio of the mechanical properties of the constituents of the system under consideration;
- as a result of the oscillation of the moving load, a parametric resonance of the system under consideration may appear and this appearance is very real in Case 2 and in similar cases.

Acknowledgments

This study was made according to the Project No 5/3, 2015: "Complex of theoretical and experimental investigations related to the study of the interdisciplinary problems of the Geomechanics" of the National Academy of Sciences of Azerbaijan.

References

Abdulkadirov, S.A. (1981), "Low-frequency resonance waves in a cylindrical layer surrounded by an elastic medium", *J. Min. Sci*., **80**, 229-234.

Achenbach, J.D., Keshava, S.P. and Hermann, G. (1967), "Moving load on a plate resting on an elastic half-space", *Trans ASME Ser. E. J. Appl. Mech.,* **34**(4), 183-189.

Akbarov, S.D. and Ismailov, M.I. (2016a), "Dynamics of the oscillating moving load acting on the hydro-elastic system consisting of the elastic plate, compressible viscous fluid and rigid wall", *Str. Eng. Mech.* **59**(3) 403-430.

Akbarov, S.D. and Mehdiyev, M.A. (2017b), "Forced vibration of the elastic system consisting of the hollow cylinder and surrounding elastic medium under perfect and imperfect contact", *Struct. Eng. Mech.,* **62**(1), 113-123.

Akbarov, S.D. (2015), *Dynamics of Pre-strained Bi-material Elastic Systems: Linearized Three-Dimensional Approach.* Springer, New York, U.S.A.

Akbarov, S.D. and Ilhan, N. (2008), "Dynamics of a system comprising a pre-stressed orthotropic layer and pre-stressed orthotropic half-plane under the action of a moving load", *Int. J. Sol. Str.,* **45**(14-15), 4222-4235.

Akbarov, S.D. and Ilhan, N. (2009), "Dynamics of a system comprising an orthotropic layer and orthotropic half-plane under the action of an oscillating moving load", *Int. J. Sol. Str,* **46**(21), 3873-3881.

Akbarov, S.D. and Ismailov, M.I. (2015), "Dynamics of the moving load acting on the hydro-elastic system consisting of the elastic plate, compressible viscous fluid and rigid wall", *CMC: Comput. Mater. Contin.*, **45**(2), 75-105.

Akbarov, S.D. and Ismailov, M.I. (2016b), "Frequency response of a pre-stressed metal elastic plate under compressible viscous fluid loading", *Appl. Comput. Math.,* **15**(2), 172-188.

Akbarov, S.D. and Mehdiyev, M., (2017a), "In the influence of the initial stresses on the critical velocity of the moving ring load acting in the interior of the hollow cylinder surrounded by an infinite elastic medium", *Proceedings of the World Congress on Advances in Structural Engineering and Mechanics, Volume of Abstracts, August-September*, Ilsan (Seoul), Korea.

Akbarov, S.D. and Panakhli, P.G. (2015), "On the discrete-analytical solution method of the problems related to the dynamics of hydro-elastic systems consisting of a pre-strained moving elastic plate compressible viscous fluid and rigid wall", *CMES: Comput. Model. Eng. Sci.,* **108**(4), 89-112.

Akbarov, S.D. and Panakhli, P.G. (2017), "On the particularities of the forced vibration of the hydro-elastic system consisting of a moving elastic plate, compressible viscous fluid and rigid wall", *Coupled Syst. Mech.,* **6**(3), 287-316.

Akbarov, S.D. and Salmanova, K.A. (2009), "On the dynamics of a finite pre-strained bi-layered slab resting on a rigid foundation under the action of an oscillating moving load", *J. Sound Vibr.,* **327**(3-5), 454-472.

Akbarov, S.D., Guler, C. and Dincoy, E. (2007), **"**The critical speed of a moving load on a pre-stressed load plate resting on a pre-stressed half-plan", *Mech. Comp. Mater.,* **43**(2), 173-182.

Akbarov, S.D., Ilhan, N. and Temugan, A. (2015), "3D Dynamics of a system comprising a pre- stressed covering layer and a pre-stressed half-space under the action of an oscillating moving point-located load", *Appl. Math Model.,* **39**, 1-18.

Akbarov, S.D., Ismailov, M.I. and Aliyev, S.A. (2017), "The influence of the initial strains of the highly elastic plate on the forced vibration of the hydro-elastic system consisting of this plate, compressible viscous fluid, and rigid wall", *Coupled Syst. Mech.*, **6**(4), 439-464

Babich, S.Y., Glukhov, Y.P. and Guz, A.N. (1988), "To the solution of the problem of the action of a live load on a two-layer half-space with initial stress", *Int. Appl. Mech.,* **24**(8), 775-780.

Babich, S.Y., Glukhov, Y.P. and Guz, A.N. (2008a), "Dynamics of a pre-stressed incompressible layered half-space under load", *Int. Appl. Mech.,* **44**(3), 268-285.

Babich, S.Y., Glukhov, Y.P. and Guz, A.N. (2008b), "A dynamic for a pre-stressed compressible layered half-space under moving load", *Int. Appl. Mech.,* **44**(4), 388-405.

Babich, S.Y., Glukhov, Y.P. and Guz, A.N. (1986), "Dynamics of a layered compressible pre-stressed half-space under the influence of moving load", *Int. Appl. Mech.,* **22**(6), 808-815.

Chonan, S. (1981), "Dynamic response of a cylindrical shell imperfectly bonded to a surrounding continuum of infinite extent", *J. Sound Vibr.,* **78**(2), 257-267.

Dieterman H.A. and Metrikine, A.V. (1997), "Critical velocities of a harmonic load moving uniformly along an elastic layer", *Trans. ASME J. Appl. Mech*., **64**, 596-600.

Dincsoy, E., Guler, C. and Akbarov, S.D. (2009), "Dynamical response of a prestrained system comprising a substrate and bond and covering layers to moving load", *Mech. Comp. Mater.,* **45**(5), 527-536.

Eringen, A.C. and Suhubi, E.S. (1975), *Elastodynamics, Finite Motion, Vol. I; Linear Theory, Vol. II*, Academic Press, New York, U.S.A.

Forrest, J.A. and Hunt, H.E.M. (2006), "A three-dimensional tunnel model for calculation of train-induced ground vibration". *J. Sound Vibr*. **294**, 678-705.

Hasheminejad, S.M. and Komeili, M. (2009), "Effect of imperfect bonding on axisymmetric elastodynamic response of a lined circular tunnel in poroelastic soil due to a moving ring load", *Int. J. Sol. Str.,* **46**, 398-411.

Hung, H.H., Chen, G.H. and Yang, Y.B. (2013), "Effect of railway roughness on soil vibrations due to moving trains by 2.5D finite/infinite element approach", *Eng. Struct.,* **57**, 254-266.

Hussein M.F.M., François, S., Schevenels, M., Hunt, H.E.M., Talbot, J.P. and Degrande, G. (2014), "The fictitious force method for efficient calculation of vibration from a tunnel embedded in a multi-layered half-space", *J. Sound Vibr.,* **333**, 6996-7018.

Jensen, F.B., Kuperman, W.A., Porter, M.B. and Schmidt, H. (2011), *Computational Ocean Acoustic*, 2nd Edition, Springer, Berlin, Germany.

Metrikine, A.V. and Vrouwenvelder A.C.W.M. (2000), "Surface ground vibration due to a moving load in a tunnel: two-dimensional model", *J. Sound Vibr.,* **234**(1), 43-66.

Ouyang, H. (2011), "Moving load dynamic problems: A tutorial (with a brief overview)", *Mech. Syst. Sig. Proc.,* **25**, 2039-2060.

Parnes, R. (1969), "Response of an infinite elastic medium to traveling loads in a cylindrical bore", *J. Appl. Mech., Trans.,* **36**(1), 51-58.

Parnes, R. (1980), "Progressing torsional loads along a bore in an elastic medium", *Int. J. Sol. Struct.,* **36**(1) 653-670.

Pozhuev, V.I. (1980), "Reaction of a cylindrical shell in a transversely isotropic medium when acted upon by a moving load", *Sov. Appl. Mech.*, **16**(11) 958-964.

Sheng, X., Jones, C.J.C. and Thompson, D.J. (2006), "Prediction of ground vibration from trains using the

wavenumber finite and boundary element methods", *J. Sound Vibr.,* **293**, 575-586.
Shi, L. and Selvadurai, A.P.S. (2016), "Dynamic response of an infinite beam supported by a saturated poroelastic half space and subjected to a concentrated load moving at a constant velocity", *Int. J Solid. Str.* **88-89**, 35-55.
Tsang, L. (1978), "Time-harmonic solution of the elastic head wave problem incorporating the influence of Rayleigh poles", *J. Acoust. Soc. Am.,* **65**(5), 1302-1309.
Yuan, Z., Bostrom, A. and Cai, Y. (2017), "Benchmark solution for vibration from a moving point source in a tunnel embedded in a half-space", *J. Sound Vibr.,* **387**, 177-193.
Zhenning, B.A., Liang, J., Lee, V.W. and Ji, H. (2016), "3D dynamic response of a multi-layered transversely isotropic half-space subjected to a moving point load along a horizontal straight line with constant speed", *Int. J. Solid Str.,* **100-101**, 427-445.
Zhou, J.X., Deng, Z.C., Hou, X.H. (2008), "Critical velocity of sandwich cylindrical shell under moving internal pressure", *Appl. Math. Mech.*, **29**(12), 1569-1578.

CC